SYNTHESIS AND INVESTIGATION OF OPTICAL AND ELECTROCHEMICAL PROPERTIES OF ORGANOBORON BASED DONOR-ACCEPTOR TYPE CONJUGATED POLYMERS

A THESIS SUBMITTED TO
THE GRADUATE SCHOOL OF NATURAL AND APPLIED SCIENCES
OF
MIDDLE EAST TECHNICAL UNIVERSITY

BY

BERRİN AYYILDIZ

IN PARTIAL FULFILLMENT OF THE REQUIREMENTS
FOR
THE DEGREE OF MASTER OF SCIENCE
IN
CHEMISTRY

JULY 2021

Approval of the thesis:

SYNTHESIS AND INVESTIGATION OF OPTICAL AND ELECTROCHEMICAL PROPERTIES OF ORGANOBORON BASED DONOR-ACCEPTOR TYPE CONJUGATED POLYMERS

submitted by **BERRİN AYYILDIZ** in partial fulfillment of the requirements for the degree of **Master of Science** i**n Chemistry, Middle East Technical University** by,

Prof. Dr. Halil Kalıpçılar
Dean, Graduate School of **Natural and Applied Sciences** _____

Prof. Dr. Özdemir Doğan
Head of the Department, **Chemistry** _____

Prof. Dr. Ali Çırpan
Supervisor, **Chemistry, METU** _____

Assist.Prof. Dr. Çağatay Dengiz
Co-supervisor, **Chemistry**, METU _____

Examining Committee Members:

Prof. Dr. Levent Kâmil Toppare
Chemistry, METU _____

Prof. Dr. Ali Çırpan
Chemistry, METU _____

Prof. Dr. Yasemin Aslan Udum
Technical Sciences Vocational School, Gazi University _____

Assoc.Prof. Dr. İrem Erel Göktepe
Chemistry, METU _____

Assist.Prof. Dr. Çağatay Dengiz
Chemistry, METU _____

Date: 12.07.2021

I hereby declare that all information in this document has been obtained and presented in accordance with academic rules and ethical conduct. I also declare that, as required by these rules and conduct, I have fully cited and referenced all material and results that are not original to this work.

Name Last name: Berrin Ayyıldız

Signature:

ABSTRACT

SYNTHESIS AND INVESTIGATION OF OPTICAL AND ELECTROCHEMICAL PROPERTIES OF ORGANOBORON BASED DONOR-ACCEPTOR TYPE CONJUGATED POLYMERS

Ayyıldız, Berrin
Master of Science, Chemistry
Supervisor: Prof. Dr. Ali Çırpan
Co-Supervisor: Assist. Prof. Dr. Çağatay Dengiz

July 2021, 69 pages

In recent years, the element boron has an important place in the studies of alternative energy sources to solve problems arising in the field of energy production. In addition to its superior properties and wide use in many industry areas, it is known that boron is integrated into conjugated organic structures. One of the current focus points of studies on alternative energy sources is polymers with semiconductor conjugated structures and small organic molecules. In this study, boron units were embedded in a conjugated structure that were synthesized starting from pyrazine via post-borylation strategy. It is aimed to investigate the role of intramolecular boron-nitrogen (B-N) coordination bonds on the conformation of the conjugated systems and their electronic structure. The synthesis of boron-containing polymers was carried out by Suzuki-cross coupling reaction followed by the post-borylation method. Borylated polymer (**P1B**), stablized by the phenyl unit, has a lower LUMO energy compared to the polymer without the boron unit (**P1A**) and showed a red shift of about 120 nm in emission. Photoluminescence quantum efficiency (PLQY) values are 76% for **P1A** at 510 nm and 58% for **P1B** at 630 nm. Luminance values were

recorded as 12000 cd/m^2 for **P1A** and 2000 cd/m^2 for **P1B**. Current efficiencies of **P1A** and **P1B** were recorded as 1.3 cd/A at 9.0 V and 0.3 cd/A at 9.0 V, respectively.

Keywords: Post-borylation, Photoluminescence, Conjugated Polymers

ÖZ

ORGANOBOR BAZLI DONÖR-AKSEPTÖR TİPİ KONJÜGE POLİMERLERİN SENTEZİ VE OPTİK VE ELEKTROKİMYASAL ÖZELLİKLERİNİN ARAŞTIRILMASI

Ayyıldız, Berrin
Yüksek Lisans, Kimya
Tez Yöneticisi: Prof. Dr. Ali Çırpan
Ortak Tez Yöneticisi: Dr. Öğr. Üyesi Çağatay Dengiz

Temmuz 2021, 69 sayfa

Son yıllarda enerji üretimi alanında ortaya çıkan sorunların çözümü için alternatif enerji kaynakları çalışmalarında bor elementi önemli bir yere sahiptir. Borun üstün özelliklerinin ve birçok endüstri alanında yaygın kullanımının yanı sıra konjüge organik yapılara entegre olduğu bilinmektedir. Alternatif enerji kaynakları üzerine yapılan çalışmaların güncel odak noktalarından biri, yarı iletken konjüge yapılara sahip polimerler ve küçük organik moleküllerdir. Bu çalışmada bor birimleri pirazin biriminden başlanarak sentezlenen konjüge yapıya post-borilasyon tekniği ile entegre edilmiştir. Molekül içi bor-azot (B-N) koordinasyon bağlarının, konjüge sistemlerin konformasyonları ve elektronik yapıları üzerindeki rolünün araştırılması amaçlanmaktadır. Bor içeren polimerlerin sentezi, Suzuki-çapraz kenetlenme reaksiyonu ve ardından post-borilasyon yöntemi ile gerçekleştirilmiştir. Bor eklenmiş (**P1B**) ve fenil ünitesi ile kararlı hale gelen bor içeren polimer, bor ünitesi olmayan polimere (**P1A**) göre daha düşük LUMO enerjisine sahiptir ve emisyon spektroskopisinde yaklaşık 120 nmlik kırmızı bölgeye kaymaya neden olur. Fotolüminesans kuantum verimliliği (PLQY) değerleri 510 nm'de **P1A** için %76 ve

630 nmde **P1B** için %58dir. Parlaklık değerleri **P1A** için 12000 cd/m^2 ve **P1B** için 2000 cd/m^2 olarak kaydedildi. **P1A** ve **P1B'**nin akım verimleri sırasıyla 9.0 Vda 1.3 cd/A ve 0.3 cd/A olarak kaydedildi.

Anahtar Kelimeler: Post-borilasyon, Fotolüminesans, Konjüge Polimer

To my beloved family…

ACKNOWLEDGMENTS

First, I would like to thank Prof. Dr. Ali Çırpan, who is my supervisor during my graduate education, for the opportunities he provided me, for always being there for me and for his endless support in every subject. I am very lucky to have such a friendly, sincere, and kind-hearted advisor and there are no words to express the respect and gratitude I have for him.

I would like to thank my dear co-advisor Assist.Prof.Dr. Çağatay Dengiz for always supporting me and teaching me never to give up. I can't tell you how grateful I am that he tirelessly listened to me and gave sincere advice. I would like to thank him for his scientific expertise and for always creating a plan B, which made me progress academically.

I would like to thank Prof. Dr. Levent Toppare for his unique and valuable guidance.

I would like to thank Prof. Dr. Yasemin Aslan Udum and Assist.Prof.Dr Şerife Özdemir Hacıoğlu for the unique information they taught me about electrochemical studies and for the patience they showed me during this process.

I would like to thank Sultan Taşkaya Aslan very much for her valuable synthesis information and the peace she provided in the laboratory environment.

I would like to thank my dear project friend Yeşim Abacıoğlu for laughing and crying together, sharing our lives sincerely and never making me feel alone. Thank you so much for the beautiful, precious, and eternal friendship I have had.

I would like to thank Eda Alemdar Yılmaz for photovoltaicstudies and most of all, for always being kind.

I sincerely thank my dear friends Deniz Şen Kardelen, Gülsüm Güneş and Kübra Erden, who are the most precious assets that the department has given me, for being my friends and for the precious time we spent.

I would like to thank my friend Ali Sait Güllü, who always believed in me and did not spare his support. I also thank him very much for the life advice he gave me, even though I don't apply it.

I would like to thank Gülten Özkul Atlı, Meriç Çalışkan and Merve Yıldırım for the fun times we had, for their precious friendships and for the things we shared since the first day I came to the laboratory.

I would like to thank Oğuzhan Karakurt, Selin Gülmez and Dilan Ece Dıkbıyık for making my time in the laboratory fun and valuable.

I would like to thank all the Çırpan research group members for their support and teaching. I cannot express in words the joy I feel from sharing the same environment.

I would like to thank my dear parents who always support me, respect my ideas and do their best to make my dreams come true. I would like to thank my lovely mother, who taught me to be strong and honest and always felt by my side. I am so lucky to have such a wonderful mother. I would like to thank my dear sister for listening to me, for having a good time and for understanding me better than I do. I have the coolest sister in the world, and I love her so much.

I would like to thank Boren for its financial support, for allowing us to benefit from the academic opportunities of the institute, and most importantly for its contribution to the realization of this valuable project.

TABLE OF CONTENTS

LIST OF TABLES

TABLES

LIST OF FIGURES

FIGURES

LIST OF ABBREVIATIONS

ABBREVIATIONS

PV	Photovoltaic
OPV	Organic Photovoltaic
OLED	Organic Light-Emitting Diode
OFET	Organic Field-Effect Transistor
ECDs	Electrochromic Devices
LEDs	Light-emitting diodes
VB	Valence band conduction band
CB	Conduction band
ITO	Indium Tin Oxide
PL	Photoluminescence
HTL	Hole Transport Layer
ETL	Electron Transport Layer
PEDOT	Polyethylenedioxythiophene
PSS	Polystyrene Sulfonate
$PC_{71}BM$	Phenyl-C_{71}-butyric acid methyl ester
CP	Conjugated Polymer
HOMO	Highest Occupied Molecular Orbital
LUMO	Lowest Unoccupied Molecular Orbital

V	Voltage
UV	Ultraviolet
Vis	Visible
IR	Infrared
NIR	Near-Infrared
D	Donor
A	Acceptor
E_g	Band-gap
E_g^{op}	Optical Band-gap
E_g^{el}	Electronic Band-gap
CV	Cyclic Voltammetry
$TBAPF_6$	Tetrabutylammonium Hexafluorophosphate
ACN	Acetonitrile
CE	Counter Electrode
RE	Reference Electrode
WE	Working Electrode
NBS	*N*-Bromosuccinimide
DCM	Dichloromethane
DMF	Dimethylformamide
THF	Tetrahydrofuran
NMR	Nuclear Magnetic Resonance
M_n	Number Average Molecular Weight

M_w	Weight Average Molecular Weight
PDI	Polydispersity Index
GPC	Gel Permeation Chromatography
TGA	Thermal Gravimetry Analysis
DSC	Differential Scanning Calorimetry

CHAPTER 1

INTRODUCTION

1.1 Conjugated Polymers

The polymer is a macromolecule that contains many repeating units name as a monomer. Both synthetic and natural polymers play important role in daily life due to their wide range of properties. Polymer exists in every field from synthetic plastics like polystyrene to natural biopolymers such as proteins and DNA. The high molecular weight of polymers causes it to have excellent physical properties like toughness, viscoelasticity, and elasticity. Until 1977 Hideki Shirakawa, Alan Macdiarmid, and Alan Heeger discovered polyacetylene as a conductor material after the doping process with oxidation, all polymers were insulating materials [1] . This study, which received the Nobel Prize in 2000, initiated the synthesis of many conjugated polymers and their use in the electronic and photonic fields due to their high optical and semiconducting properties.

Conjugated polymers are organic macromolecules with a backbone chain consisting of alternating double and single bonds, and their conductivity can be altered from semiconductor state to the metallic state upon doping [2]. The formation of delocalized π electrons by overlapping p orbitals results in excellent electronic and optical properties. As a result of the free movement of the delocalized π electrons along the chain, electricity is generated for the charge carriers. Therefore, polymers conduct electricity. P-doping is formed because of oxidation of the polymer by using chemical oxidizer or electrochemical method, and the population of the bonding π orbital (HOMO) decreases with the formation of holes. As the doping process occurs,

weakly bonded electrons in the system can bounce around the polymer chain, causing the polymer to generate an electrical current [3]. The biggest advantage of conducting organic polymers is that they can be processed. There has long been interested in the preparation of soluble conjugated polymers so that polymers with properties such as polymerization, purification, characterization, and processability to be carried out in solution are defect-free and form thin films. Due to their chemical structure, conjugated polymers are insoluble in most organic solvents, so many scientific fields have endeavoured to improve their solubility and hence processability. To eliminate this disadvantage, the design of suitable monomers and the addition of solubilizing side chains on the conjugated backbone are the most convenient and common methods [4]. As a result of their unique properties such as processability, low cost, flexibility, lightweight, and tunability organic conjugated polymers have gained an important place in both the industry and the science world. In recent years, due to their electrical conductivity and conjugate structure conjugated polymers have gained a wide place in application areas such as Organic Solar Cells (OSCs), Organic Light-Emitting Diodes (OLEDs), Electrochromic Devices (ECDs), Organic Field Effect Transistors (OFETs) [5]. Figure 1.1. indicates commonly used conjugated polymers in optoelectronics.

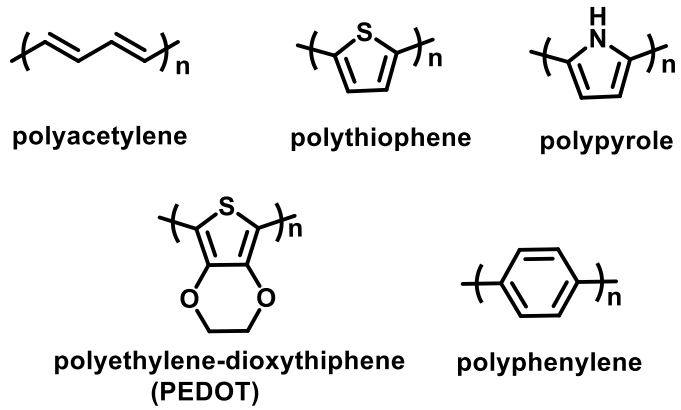

Figure 1.1. Common conjugated polymers in the literature.

1.2 Band Theory

Band theory is used to describe the behaviour of electrons in a solid and this theory contributes greatly to explain many phenomena such as electrical resistance and optical absorption. According to this theory, the material always has energy bands to be filled with electrons and energy bands where electrons cannot be found. Materials are divided into 3 groups in terms of conductivity which are metals, semiconductors, and insulators. The main difference between them is bandgap which is the distance between the valence band (VB) and the conduction band (CB). The valence band is the highest energy band with electrons in it, while the conduction band is the lowest energy band without electrons [6]. The bandgap is also expressed as the minimum energy needed to excite an electron from the VB to the CB.

Most solids are insulators, and band theory means that there is a large gap between the energies of valence electrons and the energy (CB) where electrons can move freely through the material. The doping of insulators can change their optical properties, while their conductivity cannot be affected due to the large energy gap. Contrary to the situation in insulators, the conductivity of semiconductors increases via doping, and this is the basis of solid-state electronics [7]. The distance of the semiconductors between the VB and the CB is between the insulators and the conductors, so electrons can jump from the VB to the CB. Intrinsic and extrinsic are the two types of semiconductors. An intrinsic semiconductor is a type of semiconductor that has not undergone any doping process. For each electron that jumps to the conduction band, a freely movable hole is formed instead of the electron diminishing in the valence band, resulting in a very low conductivity level [8]. Extrinsic semiconductors are formed by adding small amounts of impurities to intrinsic semiconductors. There are two types of extrinsic semiconductors originating from the doping type: atoms with an extra electron (n-type for negative, from group V, such as phosphorus) and atoms with one missing electron (p-type for positive, from group III, such as boron). The n-type doping increases the number of electrons available to increase the conductivity of the semiconductor material, while

the p-type doping increases the number of holes available [9]. According to the band theory, metals are unique materials with good conductivity, and this is the result of the valence electrons being completely free. The valence band of the metals and the CB overlap so that at least some of the valence electrons can move through the material, which is why they conduct electricity well.

The band gaps of conjugated polymers used for photovoltaic applications must be well-tuned because the well-tunning band gap and molecular structure determines their optoelectronic properties. The most critical point for conjugated polymers to be used in photovoltaic studies is their high absorption coefficient in the visible region and this can only be achieved by reducing the band gap. Figure 1.2. shows the band gap of insulators, conductors and semiconductors.

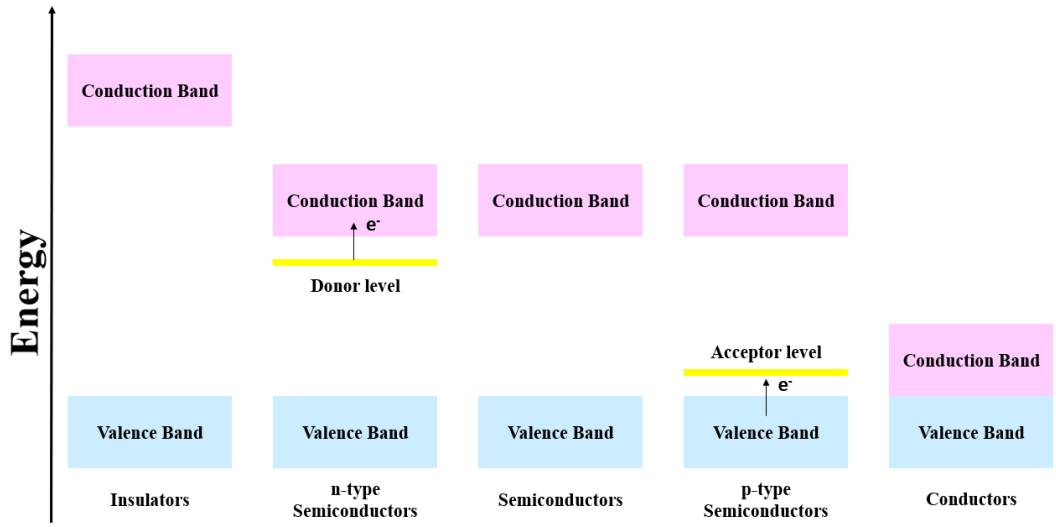

Figure 1.2. Energy bands of insulators, semiconductors and conductors

1.3 Integrating Main Group Elements Into Conjugated Polymers

Contrary to inorganics, the most widely used method in the creation of environmentally friendly organic devices is to include the main group elements in the p-conjugated scaffold. The sp^2 hybridizing boron is an efficient choice as it has an empty p_z orbital that can participate in the π conjugation. Boron doped molecules

generally exhibit impressive fluorescence and have advanced charge-transport characteristics [10]. In recent years, boron-containing π-conjugated materials have attracted the attention of the many study areas thanks to the unique properties created by the p-π* conjugation between the empty p orbital of boron and the π* orbital of the π conjugated structure. Because of its unique photophysical properties, this material class has come to the fore especially in optoelectronic applications. Within the integration of the boron unit, the boron centre can be embedded within the main chain of the conjugated polymer or added to the side chain or chains. In terms of the amount of coordination, it is grouped under two main headings as three coordinates and four coordinates. Extensive work in these two classification areas has led to the development of new and diverse synthetic methods for boron-containing conjugated polymers [11].

1.3.1 Boron-Doped Molecules for Optoelectronics

Conjugated systems containing boron units have become a new research subject for important energy conversion application areas. Embedding boron atoms into an organic compound creates electron acceptance centres with unique optoelectronic properties due to boron's electron-deficient nature and greatly improves the performance of energy conversion devices such as (OLEDs), (OPVs), and (OFETs) [12]. The presence of an empty p orbital on boron that can overlap with an organic π system is the most characteristic feature of three-coordinated organoboranes. The p-π interaction, which leads to favourable electron transport capabilities, provides linear and non-linear optical properties as well as the use of boron-containing molecules as emission and electron transmission materials in optical devices. In the early 1990s, Chujo et al. synthesized a large number of polymers carrying a boron atom in the main chain. The first stable boron-containing polymer was formed by the reaction of mesitylborane with aromatic diynes via hydroboration [13].Another boron-containing polymer reported is a polymer containing a ruthenium-phosphine complex together with boron centres performed by hydroboration polymerization of

a tetrayne-type monomer containing mesitylborane and ruthenium phosphine complex. It has been noted that the band due to the dπ-pπ transition of this polymer shifts to 141 nm red compared to the ruthenium molecular compound due to the push pull effect between the ruthenium and the organoboron unit, and the expansion of the π conjugation [14].

1.3.2 Characteristic Properties of Boron

sp^2 hybridized boron is one of the electron-withdrawing groups due to unoccupied orbitals. Boron-containing π conjugate structures are aromatic or through the overlap of p_z orbitals perpendicular to the plane of conjugated units, electrons delocalize throughout the molecule, and this explains successful application of materials in optoelectronic devices. Boron has enough electrons to fill three sp^2 orbitals with three adjacent units which will only make three s bonds, and empty p_z orbitals to participate in π conjugation with aromatic systems showed Figure 1.5. Additional conjugated units or structural constraints are the most appropriate methods to maximize the p-conjugation and stabilize the boron doped p-conjugate system [15]. The characteristic properties of the boron element can be grouped under three main headings, and these are: electronic properties i.e. due to empty p_z orbital delocalization of π electrons, nuclear properties i.e. ability of neutron capture since boron has two isotopes, one of them has a large cross section for neutrons and ability to react with oxygen to form boron trioxide(B_2O_3) or boron-nitride ceramic materials in B-N containing compound case [16].

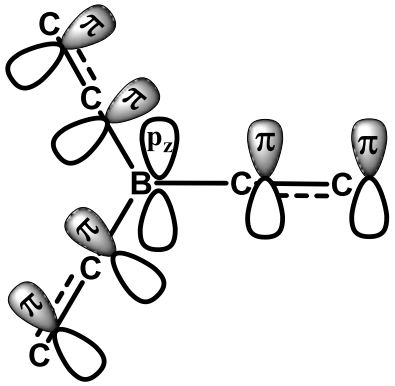

Figure 1.3. Interaction of p_z orbital of boron and π orbitals of conjugated systems

1.3.3 Characteristic Properties B←N Bridged Molecules

Molecules containing B-N have different properties from their isoelectronic several carbon allotropes (e.g., graphene, diamond, nanotubes) due to their polarized B-N linkages [17]. Large electronic band gaps (5.9 eV in hexagonal B-N) and chemical inertness are two characteristics of molecules containing b-n, making this boron nitride an interesting field of study for the electronic applications in the construction of devices based on B-N / graphene heterostructures [18].However as an electron-deficient building block, due to fixed planar configuration, molecules containing bn have the LUMO and HOMO energy levels at low levels [19]. Incorporation of B-N units into π conjugated polymers significantly changes HOMO-LUMO energies, causing them to be used as both acceptor and transmitter for organic photovoltaics.

1.4 Research Interest

1.4.1 Post-borylation

In addition to classical polymer science, variety of new polymerization techniques are available in modern polymer science for the direct synthesis of polymers containing different functional groups. However, there are still limitations since many functional groups inhibit polymerization or cause side reactions. Post-polymerization modification, also called polymer-analog modification, is another method to beat these limitations. This strategy supports the integration of a large number of functional groups that are inert or unstable to the polymerization conditions but allow a quantitative conversion within the next reaction step. Thus, studies emerge the incorporation of a wide variety of functional groups with the identical average polymer grade but also variable side chain properties [15]. The success of this system relies on successful conversions achievable under mild conditions, the chance it creates against functional groups that are desired and inert or unstable to polymerization conditions, and orthogonality of the post-polymerization method reactions [20].

The study of Daniel et al. published in 2017 is proof of the applicability of the post-polymerization borylation method to get conjugated polymers with high emissivity and low band gap properties. Within the aforementioned study, BCl_3, which is a frequently preferred Lewis acid within the literature, was used as a boron source within the integration of boron unit into conjugated polymers containing benzothiadiazole and fluorene within the electrophilic C-H borylation method, and diphenylzinc was want to provide a stable structure. This study was repeated for different boron unit percentages, and it was aimed to determine an optimal percentage for the integration of the boron unit into the conjugated polymer. There are two methods within the literature as proof of the post borylation attempts. The first of those is to use GPC to determine the molecular weight increase upon addition

of the boron unit. Another is that polymers containing boron units show a bathochromic shift of over 100 nm [21].

1.4.2 Suzuki Cross Coupling Reaction

The Suzuki or Suzuki-Miyaura reaction in which organoboron compounds and organic halides or triflates react in the presence of a palladium catalyst to form carbon-carbon bonds is one of the best known and most frequently used crosslinking reactions [22]. In 1981, Suzuki and Miyaura performed the first Suzuki type crosslinking reaction between phenylboronic acid and haloarenes. Since the electronegativities of boron and tin used for transmetallation in Stille coupling are similar, Suzuki cross linking reaction is often compared with the Stille cross linking reaction. It is used for the same purpose in both reactions, to generate new carbon carbon bond, and proceed via a similar mechanical cycle with a similar content [23]. Another common feature of these two methods is that they offer mild reaction conditions that tolerate a wide variety of functional groups. Suzuki coupling reaction is also used in the industrial synthesis of highly complex pharmaceuticals in addition to academic studies since the aryl-aryl structure is an important building block in pharma industries. Reasons for the widespread use of the reaction are the broad functional group tolerance, low toxicity of organoborons and commercial availability mild reaction conditions, and the use of water as a solvent or auxiliary and ease of use of products and by-products [24]. In recent years, the use of water in the reaction medium has become a topic of great interest in terms of environmentally friendly working areas. Compared to organic solvents used in the Stille crosslinking reaction using palladium catalysts, water is non-flammable, cheap, non-toxic, and abundant solvent. Besides, inorganic materials with high water solubility can be easily separated from the organic part. A disadvantage of the aqueous catalyst is the disposal of contaminated waste water, which can be reduced by reducing the catalyst amount or by recycling the catalyst. However, effective Suzuki catalysis in aqueous

media is often restricted by the limited substrate solubility or the reduced stability of the catalyst in water so phase transfer catalysts are used to dissolve non-polar substances and increase their concentration in the reaction medium. Generally, the use of additives such as reverse phase transfer catalysts (PTC, eg calix [n] arenes) or surfactants (e.g. tetrabutylammonium bromide (TBAB) and sodium dodecyl sulfate (SDS)) to increase catalytic activity has already been successfully utilized [25]. The Suzuki cross-linking reaction mechanism starts with the oxidative addition of organohalide to Pd (0) to form a Pd (II) complex. A molecule of the hydroxide or alkoxide replaces the halogen bound to palladium, while the other attaches to the organoborane to form the borate unit that makes the R group more nucleophilic. Borate transmetalation continues with the R group replacing the halogen anion in the palladium complex. Finally, the reductive elimination creates the desired bound structure and reactivates the palladium catalyst, and the cycle is repeated [26].

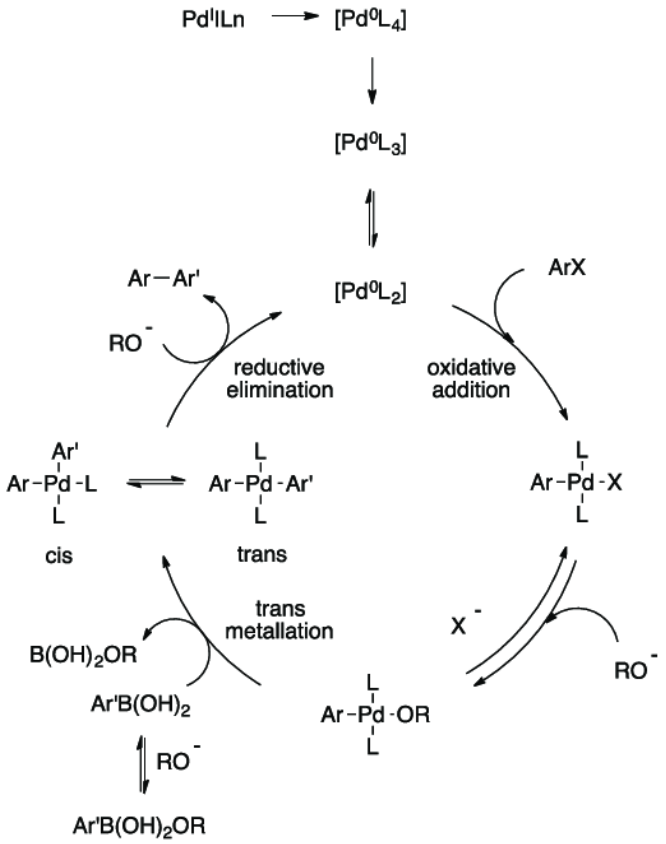

Figure 1.4. Proposed mechanism for Suzuki cross coupling.

1.4.3 Fluorene Moiety

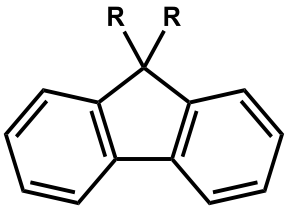

Figure 1.5. Structure of fluorene unit

Fluorene has a structure that contains two benzene groups connected to each other via carbon-carbon bond and methylene bridge and is insoluble in water and soluble in most organic solvents (Figure 1.7) [27]. Due to adjacent methylene bridge, the two phenyl rings forced to be a planar and thus the overlap of the π orbitals are provided [28]. Polymers with rigid and bulky fluorene units are soluble polymers that can show high optical and thermal properties [29]. Alkylated fluorene is widely used as a donor monomer or fluorescent molecules with applications in polymers, electronic devices, sensors, and photochromic materials [30].

1.4.4 Pyrazine Moiety

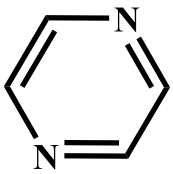

Figure 1.6. Structure of pyrazine unit

Pyrazine is a six-membered heterocycle with two nitrogen atoms with a solid planar conjugate structure. due to its electron-poor character, this structure can be used as an electron-withdrawing molecule in push-pull structures (Figure 1.8) [31]. Additionally, it's preferred for sensing applications because of its ability to undergo protonation, hydrogen bond formation and chelation of the nitrogen atom. The push-pull derivatives of pyrazine are known for their strong positive

solvatochromism and halochromic properties. Some pyrazine fluorophores are used as fluorescent protein sensors and a few pyrazine derivatives as emitting layers in organic light-emitting diodes or as chromophores in dye-sensitized solar cells [32].

1.5 Introduction to OLED Technologies

Organic light emitting diodes (OLEDs) are about to become the number one technology of choice for high-quality display panel and environmentally friendly solid-state lighting, thanks to their unique features such as mercury-free production, energy savings, wide viewing angle, fast response, elevated contrast and colour quality of higher rank [33].OLED, with its very simple definition, is a light emitting structure consisting of an organic film placed between 2 charged electrodes, a metal cathode and a transparent anode, which is generally made of glass [34].

1.5.1 Brief History of OLED

In 1965, by using anthracene, Helfrich and Schneider were discovered the first electroluminescence in organic structures in history and they made the beginning of a breakthrough work that will be reported in the literature in the future [35].

Figure 1.7. The first electroluminescence in organic structures device architecture

Until the first efficient low voltage organic electroluminescence was developed by Tang et al. in Kodak company in 1987 (Figure 1.9), the electroluminescence device that was put into practice could not be designed due to the very high voltage (~100 V) of the first organic electroluminescence made from anthracene. This study embodies one of the most basic principles for the practical applications of OLED technology, with the use of organic heterostructure, OLED as it is known today [36]. In addition to having the first OLED architecture with a double layer structure, this study in 1987 also achieved light emission at about 2.5 V and a high brightness (above 1000 cd/m^2) at a driving voltage of less than 10 V [37]. The secret of this work is explained by a model consisting of separate carrier transport layers, one of which is the hole transport layer, and the other is the electron transport layer, and these layers are equivalent to n- and p-type semiconductors, and recombination and light emission occur in the middle of the organic layers [38]. From the cathode, which is silver, and the anode, which is ITO, electrons and holes are injected into the electron and hole transport layers and as a result of this injection, the radiative combination of electrons and holes occurs in the Alq_3 layer. When we came to 1990, an electroluminescence using 100 nm thick poly (p phenylene vinylene) (PPV) films, that is, a conjugated polymer heterostructure called PLEDs was produced by scientists at Cambridge University. Pioneer study by S. R. Forrest, M. E. Thompson

and their groups on phosphorescent OLEDs from the late 1990s to the early 2000s exceeded the 25% internal quantum efficiency η_{int} of fluorescent OLEDs and significantly increased the efficiency of OLEDs [39].As it is known, single excitons, which make up one fourth of all excited states, produce light for fluorescent organic materials, while triple excitons, which make up three-fourths, are almost completely lost by non-radiative decay. however, phosphorous organic molecules containing heavy metals in the centre such as platinum and iridium produce light from both triple and single excitons with a fast and efficient intersystem crossing (ISC). Thus, thanks to phosphorescent OLEDs (PHOLEDs) with power efficiency of over 100 lm/W, OLED technology has become increasingly competitive as a next-generation technology for both flat panel displays and solid-state lighting [40].

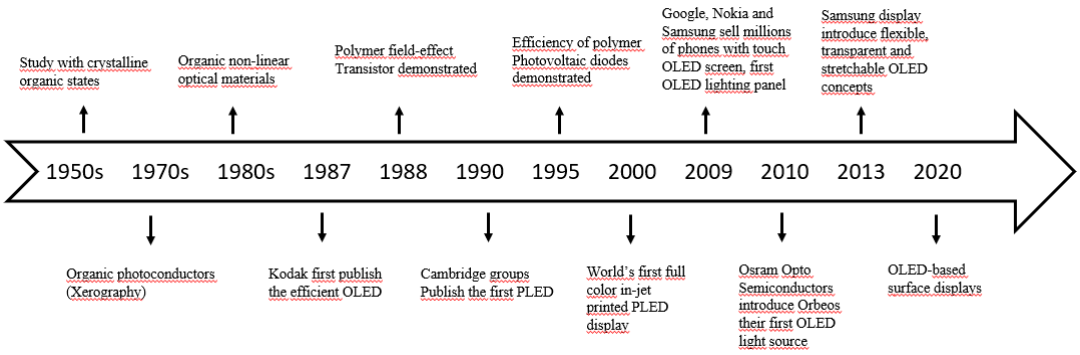

Figure 1.8. Timeline of OLED technologies

1.5.2 Electronic process

One of the most characteristic features of conjugated polymers is the delocalized electrons along the π orbital, which is responsible for their electronic properties. The charge mobility of the conjugated polymers is affected by the electronic environment and structural relaxation of the surrounding atoms resulting from any fundamental excitation of the π-bonds. As a result of the overlapping of two atomic orbitals, they are bonding and antibonding molecular orbitals [41]. The p_z electrons in the structure of conjugated polymers are delocalized on the chain by order change between single double and triple bonds. The Highest Occupied Molecular Orbital (HOMO) is the

highest electron-filled molecular orbital where electrons accumulate in the ground state, and the Lowest Unoccupied Molecular Orbital (LUMO) is the lowest vacant electron π* (anti-bond) orbital. The difference between the HOMO and LUMO energy levels is called the band gap and has values in the visible spectrum range of 1.7 to 3.2 eV for typical conjugated polymers [42].The reason why conjugated polymers can be used in various applications such as OLED and OPV is that they can be excited optically or electrically. The reasons for this excitation are direct absorption of incoming light or injecting and removing charges by means of opposite electrode contacts [43].

1.5.2.1 Luminescence

Luminescence is the emission in the optical range of visible, ultraviolet or infrared light, which is more than the thermal radiation emitted by the substance at a certain temperature and continues after absorbing the excitation energy, which is more than the period of the light waves [44]. Luminescence is inherent to each state of aggregation like gases, liquids, crystalline or amorphous solids, polymers, glass, and organic and inorganic substances [45]. In most organic substances, organic molecules have the property of luminescence both the dissolved state and the molten state. Luminescence is a type of radiation that is not in equilibrium. To produce radiation, one or another form of energy must be transferred to the luminescent material in the form of quanta of light with a higher or lower loss. Several different types of luminescence occur, depending on the excitation method of the material [46].

1.5.2.2 Electroluminescence

Electroluminescence is a phenomenon that generally occurs as a result of radiative recombination of electrons and holes in semiconductor material. Also, excited electrons release their energy as photons, that is, light. Electroluminescent materials

emit light in response to the application of an electric current and a strong electric field [47]. This phenomenon is applied in imaging devices, which can be divided into two categories, the first is low-field devices known as light-emitting diodes (LEDs), produced by electron-hole pair recombination in the p-n junction of light, and the other is that the effect of high-energy electrons stimulates luminescent centers of phosphor-containing materials and this excited state relaxes, they are high field devices where EL emission is obtained [48].Before recombination, p-n junctions can be formed by doping materials to separate electrons and holes, which usually occurs in electroluminescent semiconductor devices such as LEDs, or by excitation of high-energy electrons accelerated by a strong electric field which usually occurs the phosphor on the electroluminescent screen [49].

1.5.2.3 Photoluminescence

Photoluminescence (PL) is one in all many sorts of luminescence and therefore the reason it starts with photo is photo excitation, that is, photons excite electrons to the next energy in an atom. To define it briefly, it is the light emission resulting from the irradiation of a substance with another light. This phenomenon is named fluorescence or phosphorescence, depending on the time difference after luminescence created by luminescence [50].The emitted light is mostly within the visible region but sometimes within the ultraviolet or infrared spectral region. Considering semiconductors, PL is an optical phenomenon that emits incoming light by absorbing light that has an energy higher the energy band gap of the semiconductor [51].The PL mechanism is explained because the excited electrons formed due to optical excitation return to the ground state along with the emitting photons.

Fluorescence and phosphorescence are observed in a few compounds containing highly conjugated aromatic functional groups and solid molecular structures. As shown in figure, absorption of excitation light raises molecules to different excited electronic levels related multiple vibrational levels. Excited molecules at higher

energy levels first relax to lowest vibrational level of the first excited singlet state and then return to the ground singlet state by emitting fluorescent light [52]. These relaxations take place as a result of a series of small step nonradiative deactivation processes like vibrational relaxation and internal conversion. The stokes shift occurs because of the loss of non-radiative energy before fluorescence emission and refers to fluorescence with a longer wavelength than the excitation light. The stokes shift occurs due to the loss of non-radiative energy before fluorescence emission and refers to fluorescence with a longer wavelength than the excitation light. A transition from singlet to singlet is allowed as long because the transition is much probable and with a quick fluorescence lifetime of roughly 10^{-8} seconds. If the transition between systems occurs from the first excited singlet (S1) to triplet (T1) due to the overlap of isoenergetic vibration levels, it ends up within the emission of phosphorescent radiation when the excited molecule turns from T1 to S0. As is seen from the figure, the energy of the first excited singlet state is on top of the energy of the excited triplet state. This means that the phosphorescence emission encompasses a wavelength even longer than the fluorescence. Since a triple singlet transition is forbidden, the common phosphorescence lifetime (10^{-4} to 10 s) is way longer than the fluorescent lifetime [53].

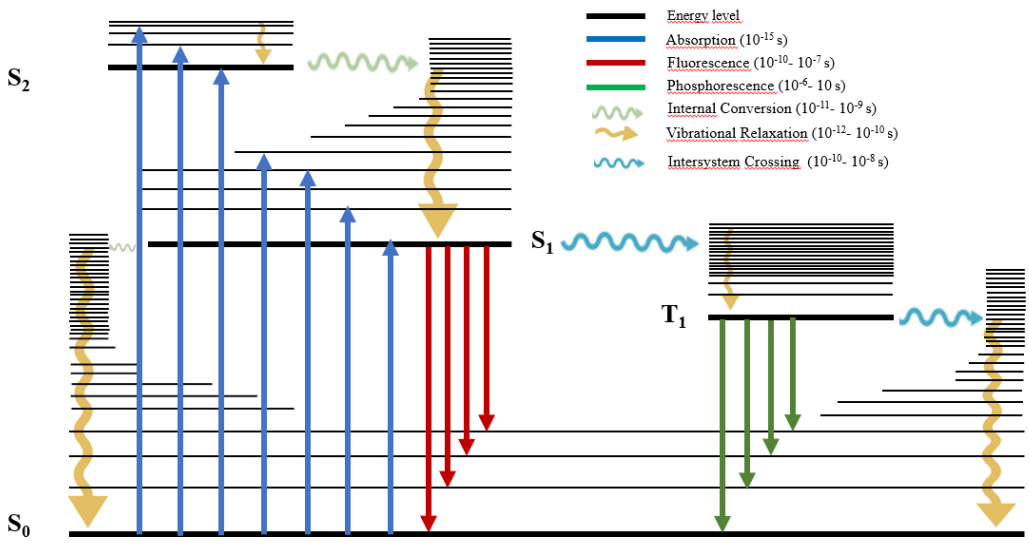

Figure 1.9. Jablonski diagram

1.5.2.4 Mechanism of energy transfer

D* represents an excited chemical while A represents a ground state chemical and energy transfer can occur without emitting photons thanks to the interaction between these two groups. In short, Forster states that the energy released from the excited donor can stimulate the ground state energy spontaneously, supported the Coulomb interaction between these two chemical groups [54]. After the donor group (D) is excited by a photon, it relaxes to the ground excited singleton state, S1 (according to Kasha's rule). When the electron returns to its state (S0), the energy is released can stimulate the donor group at the same time if the acceptor group is not too far away. This radiation-free process is termed resonance. The excited receiver emits a photon, returning to the ground state, completing this process. Since the mechanism is related to the Coulomb interaction between electrons, the relative distance between the donor-acceptor pair is also longer than the electron exchange energy transfer, i.e., Dexter Energy Transfer, which requires overlapping of the wavefunctions [55]. Only the Coulomb interaction, which needs spectrum overlap, determines the identity of the resonant energy. Independent of Forster's work, David L. Dexter proposed a mechanism by which an excited donor group and a receiver group could exchange electrons to realize the nonradiative process. Quenching, which refers to any physical process or molecular state that reduces molecular fluorescence, is that the building block of Dexter exchange energy transfer. Unlike Forster energy transfer, as can be seen from equation two, there is an exponential relationship between the gap between the donor and acceptor and therefore the reaction rate constant of Dexter energy transfer, and as this distance increases, the rate constant decreases [56]. The exchange mechanism typically occurs within about 10 Angstroms, making this transfer a short-range energy transfer.

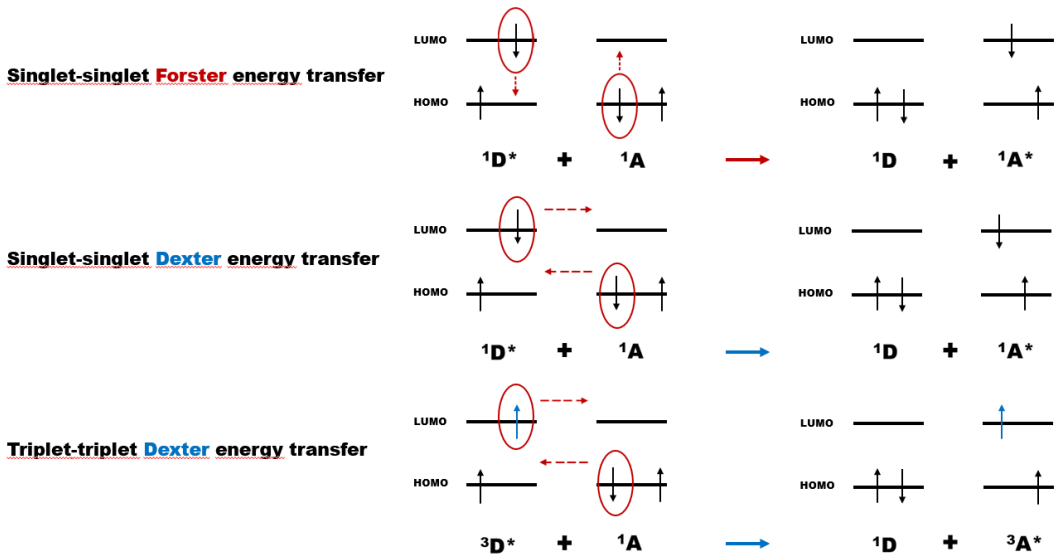

Figure 1.10. Enegy transfer mechanisms

1.5.3 Working principle of OLED

A classic OLED design consists of a layer of organic material between two electrodes, the anode, and the cathode, placed on a normally metal support. Organic molecules have highly conjugated double and triple bonds and are electrically conductive structures with the delocalization of π electrons caused by partial or complete conjugation within the molecule [57]. As mentioned in section 1.2, the conductivity of those materials is between the insulator and the conductors, and thus they are called semiconductors. Holes and electrons of closely packed, highly conjugated aromatic molecules in organic semiconductors are transported via HOMO and LUMO, respectively. Normally, both the absorption and emission of light involve the formation and disappearance of an electron-hole pair, called an exciton, as a result of electronic transfer between one molecule LUMO and HOMO. Charge carrier transport and light emission are strongly dependent to the energy of the molecular orbitals, the wave function, and therefore the thin film morphology, i.e., how the molecules are packed. Quenching an exciton from a neighbouring molecule due to packaging of organic molecules is one of the causes of loss of

function. To prevent this loss, that is, to stop quenching, the organic layer must have a particular morphological irregularity [58].

As the opposite of the working rule of solar cells, OLED starts with the application of voltage and as a result, loads move in the device. As the electrons are injected into the LUMO of the organic layer at the cathode and withdrawn from the HOMO at the anode, an electron flow occurs in the device from the cathode to the anode [59]. From another point of view the holes move from anode to cathode. This can also be interpreted as the injection of electron holes into HOMO. Electrons and holes recombine to form excitons, and since the holes are more mobile than the electrons, this merger takes place near the emission layer. The decay of this excited state leads to relaxation of the electron's energy levels and ends up in the generation of photons at a frequency determined by the band gap energy of the emitting molecules. In short, the electrical power applied to the electron and initiating this mechanism is converted into light [60].

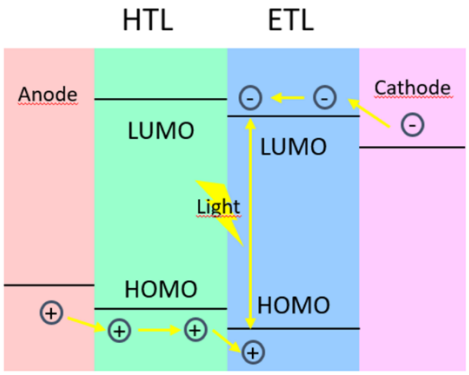

Figure 1.11. Charge transport and light generation of OLEDs

The first basic polymer-containing OLEDs in the literature had a single organic layer, such as the device synthesized by J. H. Burroughes et al., consisting of a poly (*p*-phenylene vinylene layer) [61]. However, a significant increase in yield was observed when the organic layer was designed in a multi-layered manner. The design incorporating this multi-layer structure allows the choice of materials with different electronic properties to assist charge injection at the electrodes by providing a more gradual electronic profile or preventing a charge from reaching the counter electrode

and being wasted. It has a simple double layer structure consisting of the many modern OLED conductive and emissive layers [62]. In the last 10 years, additionally the use of double-layer structure to increase efficiency, while studies on the light-emitting layer design are continuing, graduated heterojunction applications in the emitter layer have become a very important development for OLED technologies to increase both efficiency and device life. Simply put, this means that the combination of hole and electron transport materials changes across the emitter layer with the aid of the dopant emitter. In these structures, the organic layer can be mixed either uniformly in gradual grades or continuously graded. The common feature of these two methods is that although the emissive layer is basically a bipolar transport layer, the distribution of electron and hole transport materials is different [63]. This approach combines the advantages of both single-layer and double-layer emitters by improving charge injection while balancing charge transfer within the emission zone.

In the literature, indium tin oxide is often used as the anode material due to its transparency. The advantage of being transparent is that it allows the emitted light to shine and has a high working function supporting the injection of holes into the HOMO level of the organic layers. Regardless of the anode, the cathode does not have to be transparent, and metals such as barium and calcium are often preferred. and these metals have a low work function that favours electron injection into the LUMO level of the organic layer. Since both barium and calcium are in group 2A of the periodic table, they are reactive metals and to prevent degradation are often covered with a layer of aluminium [41].

1.6 Boron-doped molecules for OLED applications

Hydroboration and haloboration-phenylboration polymerization synthetic methods discovered by Chujo et al. are considered versatile synthesis methods for the integration of three coordinated boron units into the main chain of conjugated

polymers. In recent years, the hydroboration method has been employed in the development of the interesting polymer class shown in Figure 1.12. The hard and planar diboraanthracene unit utilized in this study has the property of maximizing the p conjugation of the vacant p orbitals on the boron atom. Based on the results obtained, desirable properties like strong fluorescence emission and significant bathochromic shifts within the absorption and emission spectra were observed. In addition, low LUMO energy levels and ease of reduction are accepted as electronic characteristics of the three-coordinate boron unit [64].

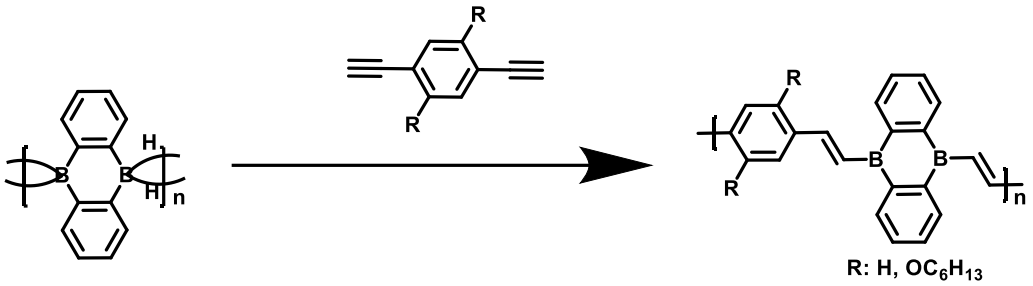

Figure 1.12. An example of post-borylation reaction

Unlike the three-coordinate species, and advantageously, the addition of four-coordinate organoboron structures to conjugated polymers results in highly stable materials. Pyrazabole, organoboron diketonate, BODIPY, and organoboron quinolate, which are shown in Figure 1.13., are tetracoordinate organoboron units that are frequently used in the construction of organoboron-containing conjugated polymers. The last three building blocks are highly emissive materials commonly used in OLEDs and fluorescent sensors [65].Therefore, its integration into polymers leads to the emergence of processable materials with very promising photophysical properties. In addition, it should be noted that the p orbital is fundamentally unsuitable for electronic delocalization due to the tetrahedral geometry of the boron centre containing all the B orbitals. Commonly Pd-catalyzed cross-linking reactions, such as Sonagashira or Suzuki coupling, are frequently used synthetic methods for such polymers [66].

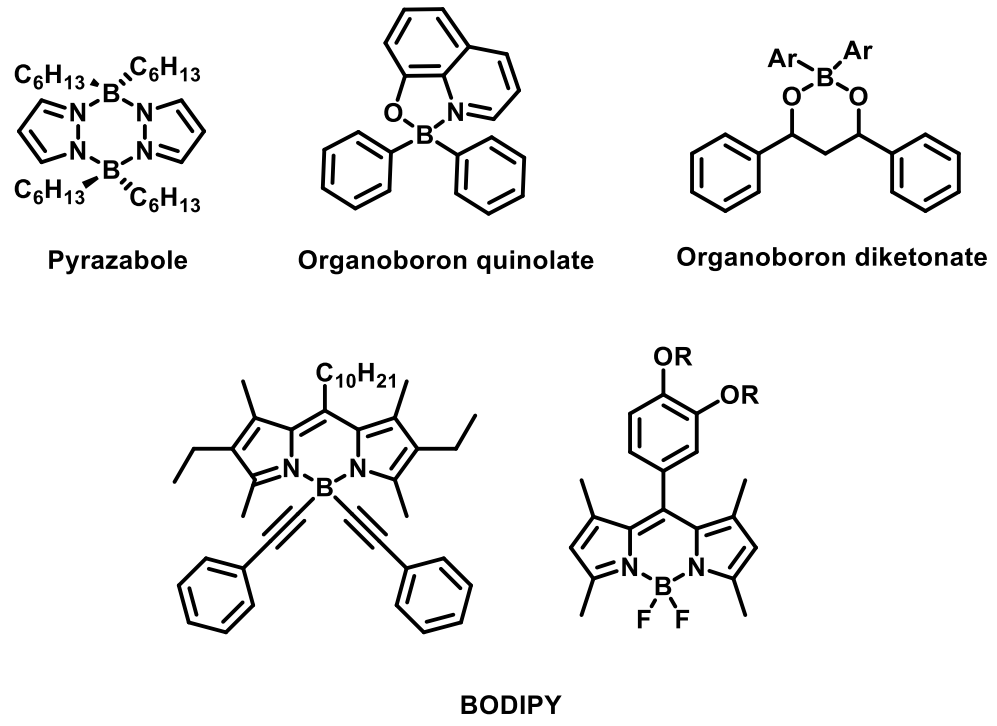

Figure 1.13. Examples of tetracoordinate organoboron units for the polymers with boron

The optoelectronic properties can be improved by incorporating main groups, such as nitrogen, phosphorus, oxygen, into mostly carbon-oriented π electron systems. In addition to these main groups, organoboron compounds have recently become a very important subject for optoelectronic applications. Structures containing three coordinate boron units synthesized by John et al. in 2018 were used in OLED studies [67]. As a result of this study, the maximum quantum efficiency was recorded as 3.4% and the maximum brightness value as 39180 cd/m^2. In the study conducted by Daniel et al. in 2017, polymers with different boron unit percentages obtained as a result of post polymerization were used for OLED applications. Photoluminescence quantum yields with optimum boron unit percentage were recorded as 44% at 700 nm [21].

1.7 Aim of study

In recent years, the boron element has an important place in studies for alternative energy sources for the solution of problems in the field of energy production. In addition to its superior properties and wide use in many areas of industry, boron is known to be integrated into conjugated organic structures. One of the current focus of studies on alternative energy sources is semiconductor conjugated polymers and small organic molecules. In this study, unique organoboron compounds with conjugated structures were synthesized starting from pyrazine. It is aimed to investigate the role of intramolecular boron-nitrogen (B-N) coordination bonds on the conformation of this monomer and its electronic structure. The synthesis of the conjugated polymer in which the boron unit will be integrated was carried out by Suzuki cross-coupling reaction. For boron unit integration, the post-polymerization mechanism, which is a new and promising method in the literature, was used. The main purpose of the study is to compare the thermal electronic optical properties of two conjugated polymers with the same chain length with and without boron unit. In the light of such studies, it is planned that boron, which has quite a lot of reserves in our country and has excellent photophysical properties, will come to the forefront in technological fields and increase its applicability.

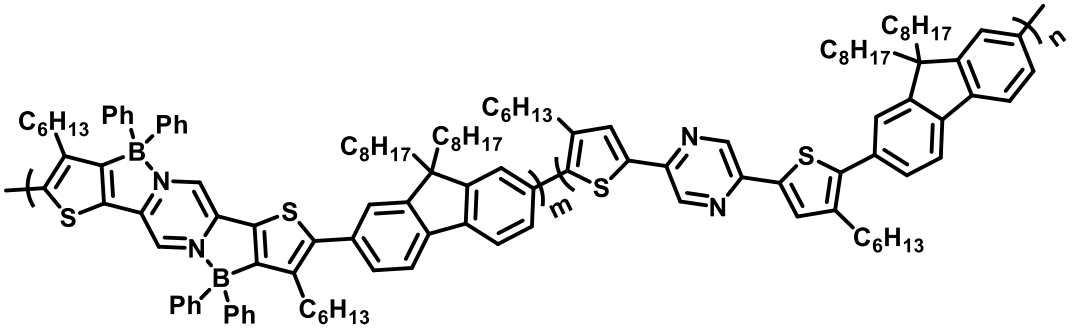

CHAPTER 2

EXPERIMENTAL

2.1 Materials and Methods

All chemicals which were used in both synthesis part and analysis part were purchased from TCI Europe except for *n*-BuLi and tributyltin chloride that were provided from Sigma-Aldrich Chemical Co. Ltd. and used without any purification unless otherwise mentioned.THF and toluene were distilled over Na/benzophenone under nitrogen atmosphere before use. DCM,$CHCl_3$, NEt_3 and DMF were dried by CaH_2 under inert atmosphere and stored over activated molecular sieves (4Å) that were kept at least 100 ^oC for 1 day before usage.Solvents used in purification process were oparated directly. All reactions were carried out under nitrogen atmosphere and classical schlenk-line methods. Merck silica gel 60 as a stationary phase with different solvent combinations was used for purification stage with column chromatography.

To identify molecular structure of compounds Nuclear Magnetic Resonance (NMR) spectroscopy was used in this study. The ^1H NMR and ^{13}C NMR spectra were measured on a Bruker Spectrospin Avance DPX-400 type spectrometer in deuterated chloroform ($CDCl_3$) as a solvent and shifts were recorded according to tetramethylsilane (TMS; $\delta = 0$ ppm) as an internal standard.

Gel permeation chromatography (GPC) by other name size exclusion chromatography (SEC), is a common method to identify average molecular weight distribution of a polymer based on difference in size of particles in solution. When the sample along with mobile phase or carrier is passes down the column larger molecules that are outside the beads moves faster than small molecules since they

are trapped in the pores of the beads. In this study GPC was used to identify number average molecular weight (M_n), weight average molecular weight (M_w) and polydispersive index (PDI) of synthesized polymers in THF (2.0 mg /mL) and using polystyrene as a reference.

Cyclic voltammetry (CV) method is used to determine electrochemical behaviour of conjugated polymers. The technique is also used both electrochemical synthesis and characterizations. to investigate both redox behaviour and electronic band gap of polymers CV method is also used. In this study redox behaviour, band gap and HOMO-LUMO energies of synthesized polymers were investigated by cyclic voltammetry with three electrodes which are Indium Tin Oxide (ITO) coated glass as a working electrode (WE), silver wire (Ag) as a reference electrode (RE) and platinum wire (Pt) as a counter electrode (CE). Dissolved polymers in $CHCl_3$ were coated on the working electrode with Omni coating gun. ITO was placed in quartz cell which is filled with supporting electrolyte and solvent mixture. Choice of solvent is crucial since solvent should dissolve supporting electrolyte and not react with electrodes. The aim of supporting electrolyte is to provide ionic conductivity. Acetonitrile (ACN) solution with 0.1 M tetrabutylammonium hexafluorophosphate (TBAPF6) were used in this study. At a constant scan rate (100 mV/s) Gamry Instrument Reference 600 Potentiostat was used to determine p- or n-type doping potentials by applying oxidizing or reducing potential. Due to doping and dedoping process, polymers were changed the colour reversibly. The graph obtained as a result of CV measurement is the current density (mA/cm^2) versus voltage (V) graph. HOMO and LUMO are calculated by the onset of oxidation and reduction potentials respectively using the following formula. The difference between HOMO and LUMO potentials give electronic band gap (Eg^{el}) of polymers.

UV-visible spectroscopy gives information about the absorption profiles both solid and solution forms of the obtained materials. In fact, the absorption vs wavelength graph obtained gives the light energy or radiation resulting from the excitation of the ground state electrons of the material to the first excited state. The obtained spectra give absorption (a.u.) vs wavelength (nm) graph that is a proof of colour change of

polymer as a result of CV analysis. Maximum absorption wavelength (λ_{max}) and optical band gap (E_g^{op}) of polymers were recorded with the help of absorption spectra. To calculate optical band gap from spectra, tangent line of point that starts absorption process of polymers is necessary. As a result of multiplying Planck's constant ($h = 6.62607004 \times 10^{-34}\ m^2\ kg / s$) by the speed of light ($c = 2.99 \times 10^8$ m/s) number 1241 in the following formula is obtained and its unit is eV.

$$E_g^{op} = 1241 / \lambda_{onset}$$

All characterizations of the produced OLEDs were carried out in the dark environment. Electroluminescence, Color, Current-Voltage, Luminance-Voltage measurements were taken using Maya spectrometer and fiber optic cable with a radius of 100 micrometers. During the measurements, voltage values were checked with the assistance of Keithley 2400 with the LabTracer program, while current values were recorded. During the electroluminescence characterization, a constant potential was applied with the Keithley 2400, while the radiation made by the OLED was collected by the fiber optic. During the colour characterization, a constant potential was applied with Keithley 2400, while the radiation made by the OLED was collected by the fiber optic. Within the luminance characterization of OLEDs, the range of 0-13 volts was scanned using Keithley 2400 source. During this scan, lumen values were recorded using SpectraSuit and current values were recorded using LabTracer.

2.2 Syntheses of Monomers and Polymers

2.2.1 Stannylation of 4-hexylthiophene [68]

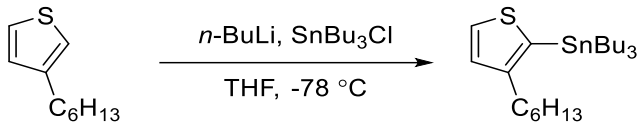

Figure 2.1. Stannylation of 4-hexylthiophene

3-hexyl thiophene (3.00 g, 17.83 mmol) was dissolved in freshly distilled 30 mL THF under inert atmosphere. *n*-BuLi (7.88 mL, 2.5 M solution in hexane) was added dropwise in the reaction medium at -78 °C over 30 minutes and the mixture were stirred for 1 hour at that temperature. Further, tributyltin chloride (5.63 mL, 19.61 mmol) was added slowly into reaction medium within 30 minutes, the mixture was allowed to warm to room temperature and reaction was stirred for 12 hours. Reaction solvent was evaporated under reduced pressure and crude product was dissolved in DCM. And then, solution was washed 3 times with brine and dried with $MgSO_4$. All volatiles were removed with rotary evaporator, pale yellow oil was obtained (7.41 g, 90% yield) and used without further purification.

2.2.2 Synthesis of 2,5-di(3-hexylthiophen-2-yl)pyrazine [69]

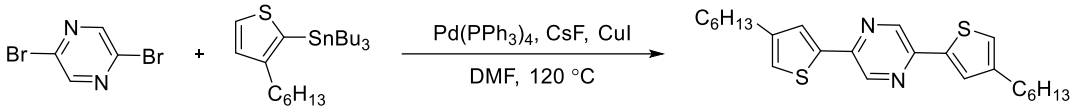

Figure 2.2. Synthesis of 2,5-di(3-hexylthiophen-2-yl)pyrazine

A 100 mL of two-necked round bottom flask was filled with 2,5-diboromopyrazine (2.00 g, 2.52 mmol) tributyl(4-hexylthiophen-2-yl)stannane (9.22 g, 20.18 mmol), CuI(64.04 mg, 336.30 µmol), CsF(12.78 mg, 84.04 µmol) and $Pd(PPh_3)_4$ (874.40 mg, 756.68 µmol) and purged with nitrogen gas for 30 minutes. Dried 30 ml DMF was added to reaction mixture and temperature increased to 120 °C and stirred overnight under inert atmosphere. After cooling to room temperature, DMF was removed under reduced pressure and residue was dissolved with DCM. Further, solution was washed with brine 3 times and dried with $MgSO_4$. All volatiles were removed with rotary evaporator, crude product was purified with column chromatography on silica gel(hexane/DCM=3:1). Product was washed with cold hexane obtaining yellow solid (2.48 g, 72% yield)

^{1}H NMR (400 MHz, $CDCl_3$) δ 0.89 (t, *J* = 6.6 Hz, 6H), 1.40 – 1.29 (m, 12H), 1.65 (m,4H), 2.64 (t, *J* = 7.6 Hz, 4H), 7.06 (s, 2H), 8.81 (s, 2H).

^{13}C NMR (100 MHz, $CDCl_3$) δ 146.14, 144.99, 141.06, 139.51, 126.72, 123.54, 31.80, 30.68, 30.56, 29.11, 22.75, 14.23.

2.2.3 Synthesis of 2,5-bis-(5-bromo-4-hexylthiophen-2-yl)pyrazine [69]

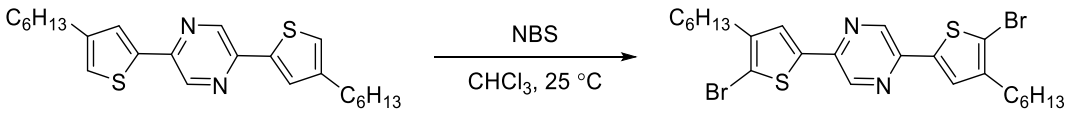

Figure 2.3. Synthesis of 2,5-bis-(5-bromo-4-hexylthiophen-2-yl)pyrazine

To a stirred solution of coupling product (1.00 g, 2.42 mmol) in 30 ml dry $CHCl_3$ dissolved 10 ml dry $CHCl_3$ *N*-bromosuccinimide (NBS) (950.90 mg, 5.84 mmol) was added dropwise with dropping funnel in dark environment under nitrogen atmosphere. After addition, system was sealed quickly and stirred 12 hours at room temperature. Reaction solvent was removed by rotary evaporator, residue was dissolved with DCM washed with brine 3 times and dried with $MgSO_4$. All volatiles were evaporated under reduced pressure, crude product was purified with column chromatography on silica gel (hexane/DCM=4:1). Yellow solid was obtained (939.04 mg, 97% yield).

^{1}H NMR (400 MHz, $CDCl_3$) δ 0.90 (t, *J* = 6.9 Hz, 6H), 1.39 – 1.30 (m, 12H), 1.63 (m, 4H), 2.59 (t, *J* = 7.6 Hz, 4H), 7.33 (s, 2H), 8.72 (s, 2H).

^{13}C NMR (100 MHz, $CDCl_3$) δ 145.35, 143.83, 138.91, 138.20, 125.92, 113.42, 31.37, 29.62, 29.18, 28.60, 22.44, 14.00.

2.2.4 Synthesis of non-borylated polymer P1A [22]

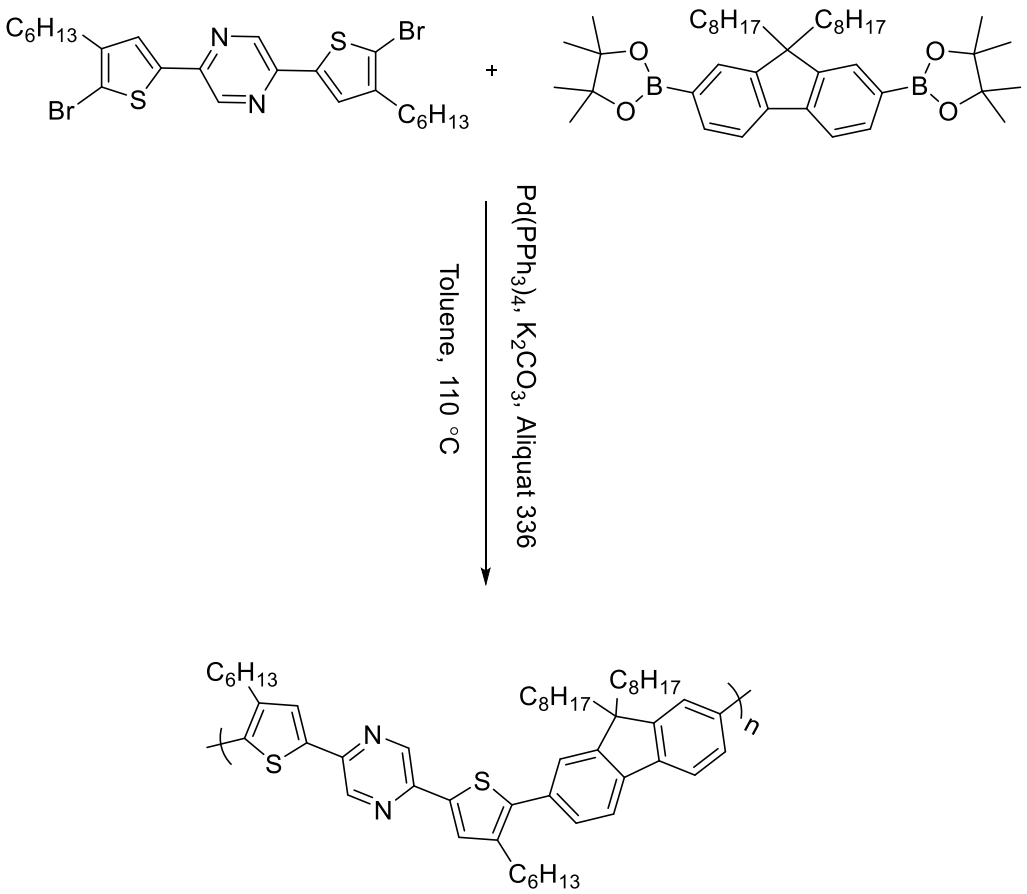

Figure 2.4. Synthesis of non-borylated polymer **P1A**

A 50 mL of Schlenk flask was filled with brominated coupling compound (600.00 mg, 1.05 mmol) and 2,2'-(9,9-dioctyl-9*H*-fluorene-2,7-diyl)bis(4,4,5,5-tetramethyl-1,3,2-dioxaborolane) (675.87 mg, 1.05 mmol) and purged with nitrogen for 30 minutes. After that, freshly distilled 20 mL toluene was added and bubbled for another 30 minutes. $Pd(PPh_3)_4$ (121.55 mg, 105.18 µmol), K_2CO_3 (2 M, 0.4 mL) and aliquat 336 (3 drops) were added to reaction mixture. And then, reaction temperature was raised to 110 °C and stirred for 72 hours. Reaction solvent was evaporated under reduced pressure and palladium scavenger (15 mg) and $CHCl_3$ were added and stirred for 1 hour. Further, after filtration process, all volatiles were removed by rotary evaporator. To remove impurities Soxhlet extraction was performed methanol,

acetone, hexane and chloroform respectively. Polymer was obtained chloroform solvent from Soxhlet extraction. Solvent was evaporated under reduced pressure and then, the residue was precipitate with cold methanol. After filtration, dark green polymer was obtained (410 mg, 47 % yield) GPC data were reported as: Number-average molecular weight (M_n) = 17 kDa, Weight-Average molecular weight (M_w) = 19 kDa. Polydispersity index (PDI) = 1.12.

2.2.5 Synthesis of borylated polymer P1B [20]

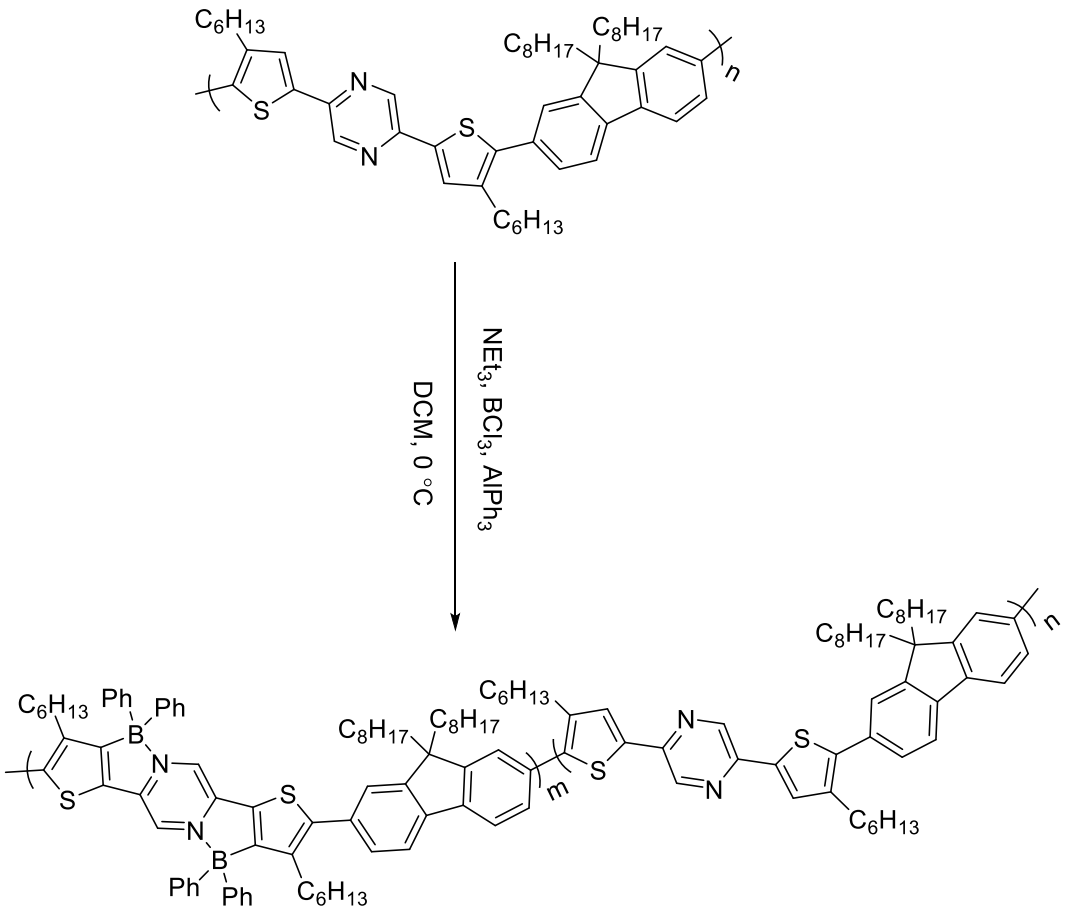

Figure 2.5. Synthesis of borylated polymer **P1B**

To a stirred solution of P1A (210 mg, 253.21 µmol) in 40 mL dry DCM freshly distilled Net_3 (53.81 mg, 531.74 µmol was added dropwise at 0 °C under nitrogen atmosphere. After stirring 10 minutes BCl_3 (1.58 mL, 1 M in toluene) was added slowly under same conditions within 15 minutes. Further temperature was allowed to raise room temperature and reaction was stirred for 12 hours. And then $AlPh_3$ (1.58 mL, 1 M in dibutylether) was added drop by drop into reaction medium and stirred for another 12 hours. After all volatiles were removed with rotary evaporator, dark red precipitate was obtained in cold methanol. Precipitate was collected by filtration and any inorganic byproducts (boron or zinc species) were dissolved in methanol. Without further purification borylated polymer as a dark red solid was

obtained (254 mg, 92% yield) GPC data were reported as: Number-average molecular weight (M_n) = 21 kDa, Weight-Average molecular weight (M_w) = 24 kDa. Polydispersity index (PDI) = 1.14.

CHAPTER 3

RESULTS AND DISCUSSION

3.1 Electrochemical Studies

Electrochemical studies were carried out with the Cyclic Voltammetry (CV) technique to determine the highest occupied molecular orbital (HOMO) and lowest unoccupied molecular orbital (LUMO) energy levels and redox behaviours of the polymers. CV is one of the successful methods used in the last few decades for the electronic band gap determination of electroactive molecular species dissolved in proper solvents [70]. Also, this technique provides information about electroactive structures corresponding to polymers in this study, redox properties, doping/dedoping mechanism, stability, energy conversion and storage. Another reason why this method is preferred is that it is a less costly and faster method when determining the electron affinity and ionization energy of structures which are the parameters correlate with the HOMO and LUMO energy levels, compared to other methods that require high vacuum [71]. Both polymers in this study **P1A** and **P1B** were dissolved in chloroform solvent and coated on the indium tin oxide (ITO) which is used as a working electrode, surface by spray coating method. Cyclic voltammograms were recorded in a 0.1 M $TBAPF_6$ acetonitrile (ACN) solution, with a three-electrode system using silver as the reference electrode and platin as the counter electrode, with a scanning rate of 100 mV/s. As seen in Figure 3.1., since both polymers **P1A** and **P1B** have n and p type doping ability, they have ambipolar character. The HOMO and LUMO energy levels of **P1A** and **P1B** were calculated as 5.46 eV/3.41 eV and 5.56 eV /3.31 eV with the onset of the oxidation-reduction potentials of the p-doping/n-doping states, respectively. The following equations are used for HOMO/LUMO energy level calculations relative to the reference energy level of the Ferrocene/ferrocenium redox couple (4.75 eV below the vacuum level).

The difference between HOMO and LUMO potentials give electronic band gap (Eg^{el}) of polymers.

$$E_{HOMO}\,(eV) = -\,(4.75 + E_{ox,onset})$$

$$E_{LUMO}\,(eV) = -\,(4.75 + E_{red,onset})$$

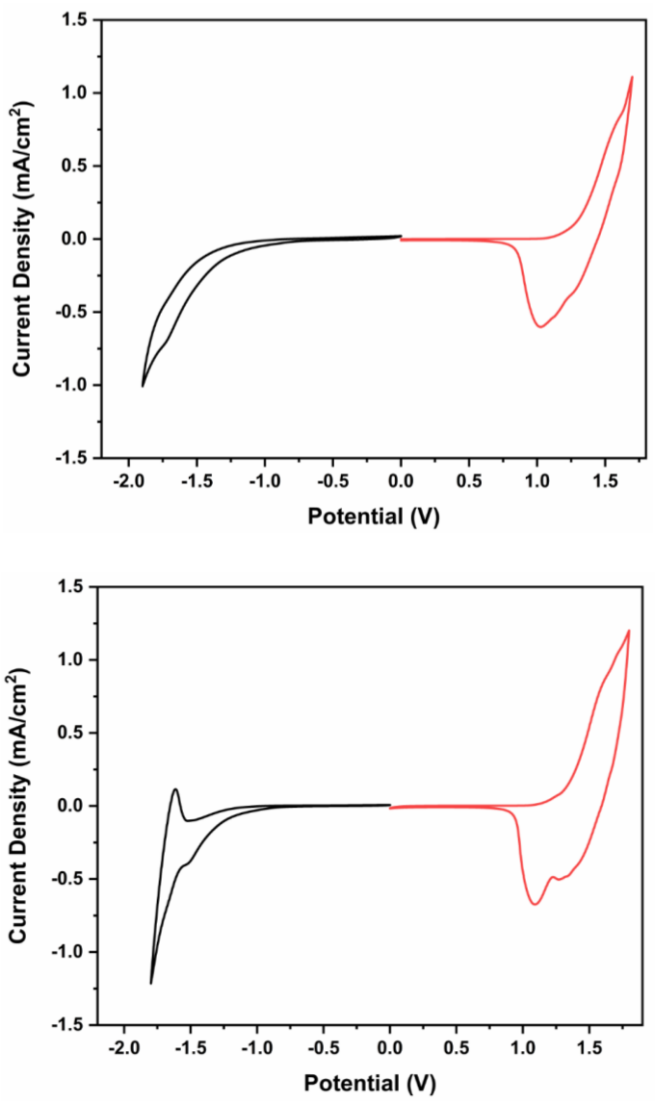

Figure 3.1 Single scan cyclic voltammograms of polymers **P1A** and **P1B** respectively in 0.1 M $TBAPF_6$/ACN electrolyte solution

All the electrochemical results are summarized in Table 3.1. The boron element integrated in the π-conjugated systems comes to the forefront by changing the electronic structures dramatically. The interaction between the empty p orbital of boron and the π*-orbitals of the conjugated system effectively reduces the LUMO level of the organic conjugated structure [72].

Table 3.1. Summary of electrochemical results of **P1A** and **P1B**

	HOMO (eV)	**LUMO (eV)**	**E_g^{el}(eV)**
P1A	5.46	3.41	2.05
P1B	5.36	3.21	2.15

3.2 Photophysical Studies

Optical studies of **P1A** and **P1B** were performed with UV-visible spectroscopy, both as a solution in chloroform solvent and as a thin film. As seen in Figure 3.2., the maximum wavelengths of **P1A** and **P1B** in solution are 435 nm and 430 nm, respectively. As can be seen from the same figure, the maximum wavelengths within the solid state are 450 nm and 455 nm. Optical band gaps were calculated using the maximum wavelengths of **P1A** and **P1B** within the solid state are 2.39 and 2.34 eV, respectively.

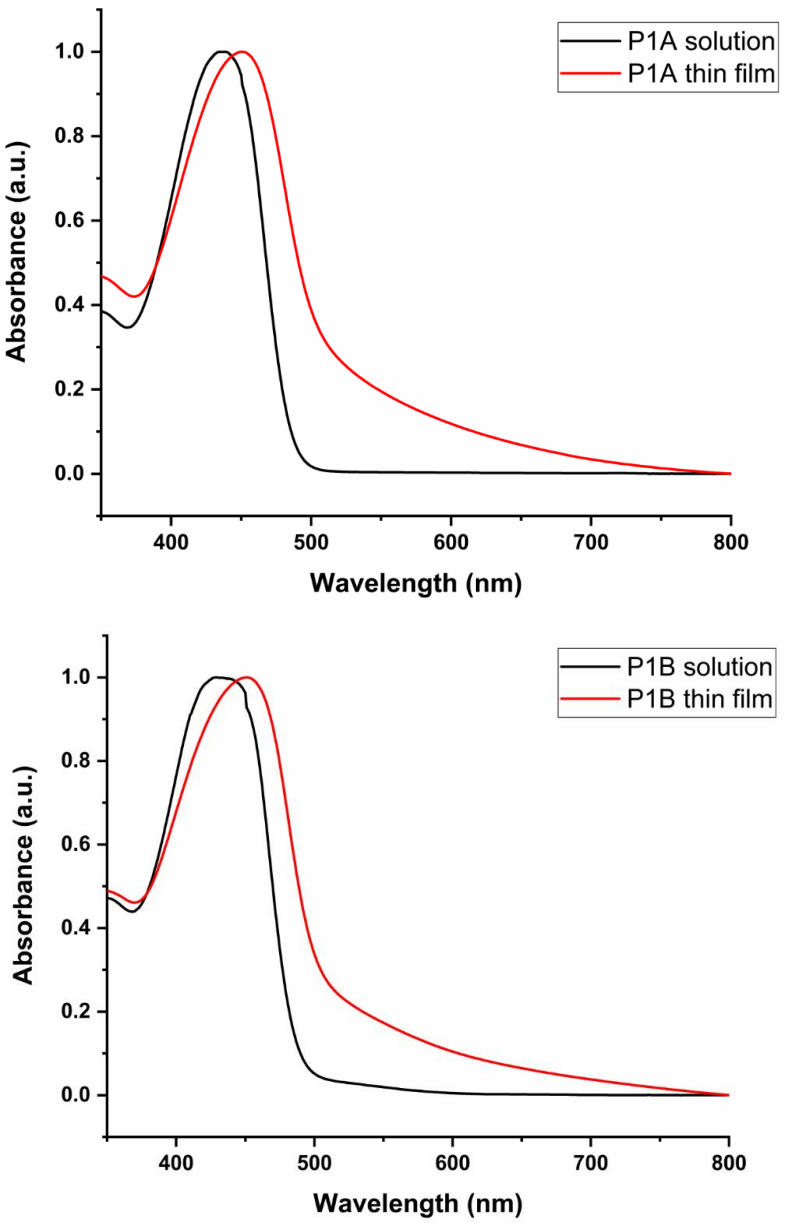

Figure 3.2. UV-Visible spectra of polymers **P1A** and **P1B** in chloroform solution and as a thin film

All these results are detailed in Table 3.2. As can be seen from the values, a red shift of about 15 nm occurred for both polymers between solution and solid-state absorptions. One of the explanations for this bathochromic shift is the increased molecular orientation because of the ordered structure of the solid state [23].

Table 3.2. Thin film and solution maximum wavelengths of **P1A** and **P1B**

	λ_{max}**(solution)**	λ_{max} **(thin film)**
P1A	435 nm	450 nm
P1B	430 nm	455 nm

Additionally, π-π stacking was observed within the solid state, because the intermolecular distance decreased, causing a red shift. Another reason for the shift to the red zone may be the lack of pre-clustering within the solution. The last and most important one is the presence of the boron unit. Although **P1A** without boron unit and **P1B** containing boron unit have very different chemical and physical structures, they have similar optical properties. This result indicates that other spectroscopic methods were needed which is why photoluminescence spectroscopy is employed. Because, as an evidence of post borylation, a bathochromic shift of 100 nm and above was observed within the visible region of the polymer containing the boron unit compared to the boron-free polymer. However, this evidence could not be observed with the UV-Vis spectroscopic method, which explains the preference of photoluminescence spectroscopy, that is directly compatible with the literature. About the electronic structure and optical processes of semiconductors was set by Photoluminescence (PL) spectroscopy, which is a non-contact, non-destructive method [73]. In this method, the light is directed towards the sample at the place where the material is absorbed, and excess energy is given off by a process called photoexcitation. The way this excess energy is dissipated by the sample is light emission or luminescence. If this happens with photoexcitation, it is called photoluminescence [74]. PL measurements were studied both as a solution prepared in chloroform solvent and as a solid state, similar to performed UV analysis. As seen in Figure 3.3., the emission maximum wavelengths of **P1A** and **P1B** are 510 nm and 620 nm, respectively. This result was expected because the effect of the integrated boron unit provides 110 nm shift towards the bathochromic region, which was observed within the emission vs wavelength graph.

As can be seen from the same figure, the maximum wavelengths from the solid state of PL of **P1A** and **P1B** were found to be 550 and 610 nm, respectively. The shift to the red region observed for both the solution and solid-state PL graphs. In addition, emission maximum wavelength of the solution form of **P1A** is 510 nm, while the solid-state emission maximum wavelength is 550 nm. The red shifted absorption observed for the solid-state measurement obtained from the UV spectroscopy was again observed for this PL measurement with respect to the result for solution form of P1A. The explanations for this are the same as the explanations for UV measurements. However, this case observed in **P1A** isn't valid for **P1B**. In other words, in contrast to the red shift between the solution in **P1A** and thin film analysis, a 10 nm blue shift was observed in **P1B**. To clarify this unexpected situation, a shift in wavelength within the emission spectra cannot be explained with the solvatochromism, although it depends on the kind of solvent used, by referring to the work carried out by Tigineh et al. [75] According to the study of Tigineh and co-workers, because of the difference between the dielectric constants of the solvents, a shift in the emission spectra was observed at larger or smaller wavelengths. Based on the PL results of the identical material measured with different solvents, a shift to the red or blue region was noted in solvents with different dielectric constants, and the reason for this is often the hydrogen bonding of various solvents with the compound. Although not directly mentioned during this study, the issue of hydrogen bonding, which consists of solvent-polymer interaction, is additionally valid for **P1B**. Since the conjugation increases as a result of boron integration, 10 nm shift to the blue region can be explained by the change in the number of hydrogen bonds.

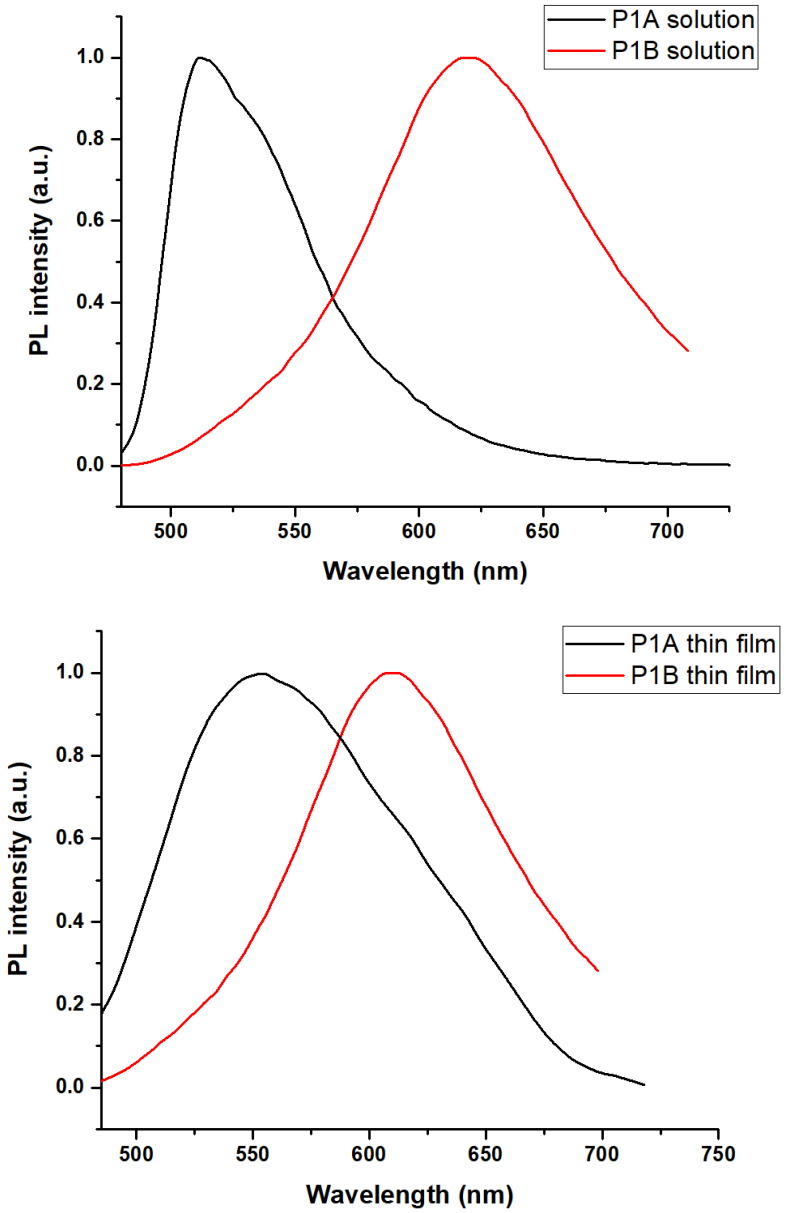

Figure 3.3. PL graphs of **P1A** and **P1B**

Table 3.3. Emission maximum wavelengths of **P1A** and **P1B**

	λ_{max}**(solution)**	λ_{max} **(thin film)**
P1A	510 nm	550 nm
P1B	620 nm	610 nm

Another reason for this unexpected blue shift can be explained as in the study of Pang et al. in 2019. In the similar molecule, the reason for the blue shift from the solution state to the solid state is attributed to the H aggregation type of interchain stacking in the solid state [12].

Another conclusion which can be extracted from these graphs is the determination of the optical band gap. Table 3.4. contains all the results. Consistent with the literature, the optical band gap was lower than the electronic band gap. The explanation for this can be the energy barrier in electronic band gap measurement. To better explain, the electrochemical redox process occurring at the interface between the electrode and the copolymer film surface causes the energy barrier [76]. The photoluminescence quantum efficiency is defined by the quantity of photons emitted per photon absorbed from the excitation source and can also be calculated by the area under the PL curves. While it is 76% for **P1A**, it is 58% for **P1B**.

Table 3.4. Optical band gaps of polymers

	λ^{onset}max (thin film)	E_g^{op} (eV)
P1A	620 nm	1.98 eV
P1B	605 nm	2.05 eV

3.3 OLED Studies

Before processing the OLED, a device architecture is designed by considering the energy diagrams of the layers. In this study, two different devices were produced using **P1A** and **P1B** in the emission layer of OLEDs. Considering the energy levels of these materials, a device architecture as in Figure 3.4. has been proposed and successful results have been obtained with this device architecture.

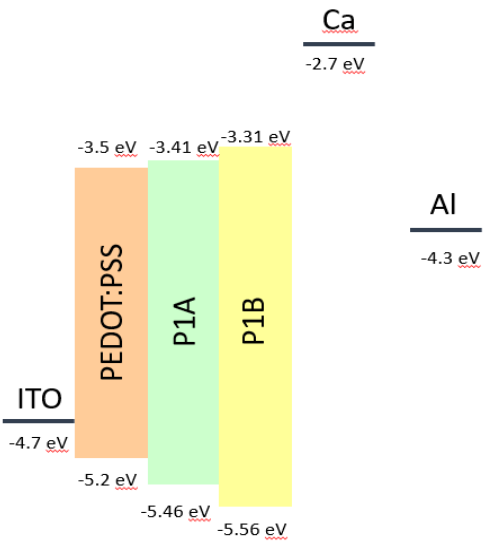

Figure 3.4. Energy level diagram for OLED device architecture

Glass substrates coated with indium tin oxide (ITO) were coated with zinc dust and then etched according to the predetermined device architecture with a 1:100 mixture of hydrochloric acid and water. Abraded ITO coated substrates were cut in dimensions of 2.45cm x 2.45cm. Abraded and cut substrates were first put into toluene and 1:100 detergent-water mixture for cleaning in an ultrasonic bath for 15 min. Then, the substrates were cleaned in an ultrasonic bath by adding water and isopropanol for 15 min each. ITO coated substrates taken from isopropyl alcohol were dried with the assistance of a nitrogen gun, and so oxygen plasma was applied for 5 min to both regulate the work function and purify from organic impurities. After oxygen plasma, the poly(3,4-ethylenedioxythiophene)-polystyrene sulfonate (PEDOT:PSS) solution was filtered through polyethersulfone (PES) filters with a pore width of 0.45 microns and coated with spin coating at 4000 rpm. Since PEDOT:PSS has a water-based structure, it was annealed at 135°C for 15 min after coating with PEDOT:PSS. In the light-emitting layer, **P1A** and **P1B** polymers were dissolved in chloroform and then covered with spin coating. Finally, Ca and Al were coated by evaporation at low pressure (~10^{-6} mbar). As a result, the device architecture is ITO/PEDOT:PSS/Light-

emitting Layer/Ca/Al. In this device architecture, ITO is the anode, PEDOT:PSS is the hole transport layer, Ca and Al are the cathode.

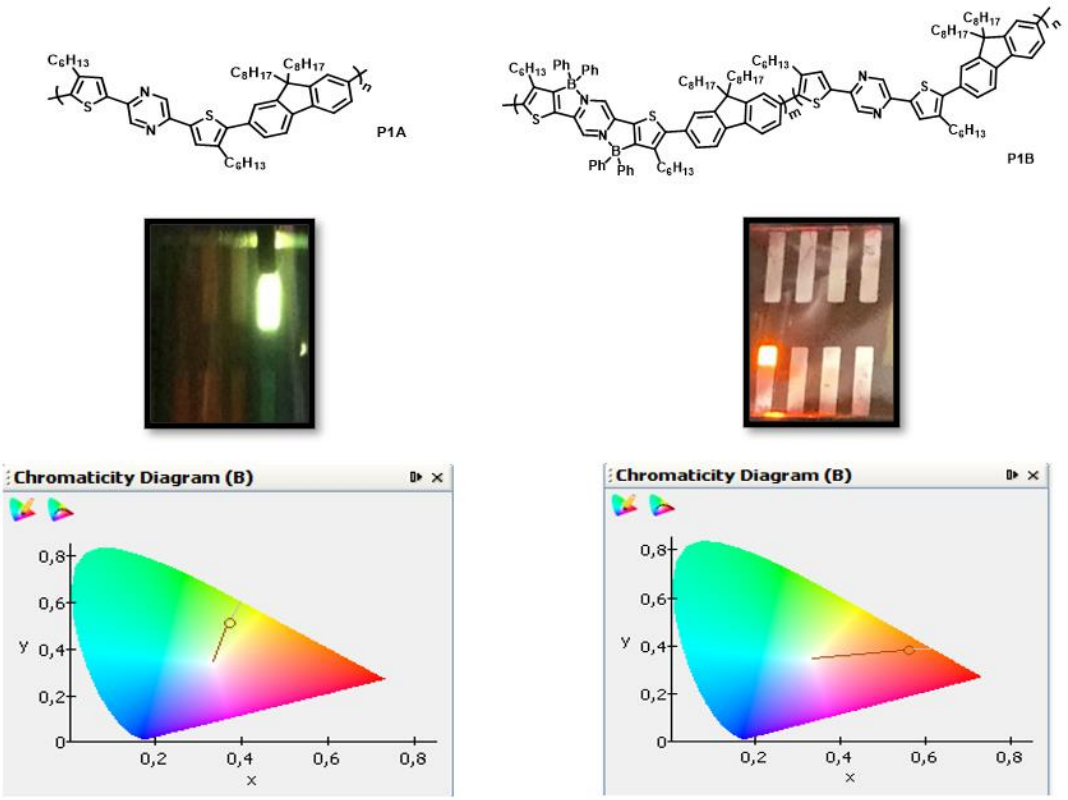

Figure 3.5. Photographs and colour gamuts of the polymers

In figure 3.5., there are photographs of the polymers used in the light-emitting layer as the devices irradiate, and the colour gamuts were obtained according to the results of this radiation. As can be seen from this figure, the colour of the **P1A** is green, while the polymer obtained by the integration of boron has an orangeish red colour. This colour difference is another proof of the physical and chemical change created by the integration of the boron unit.

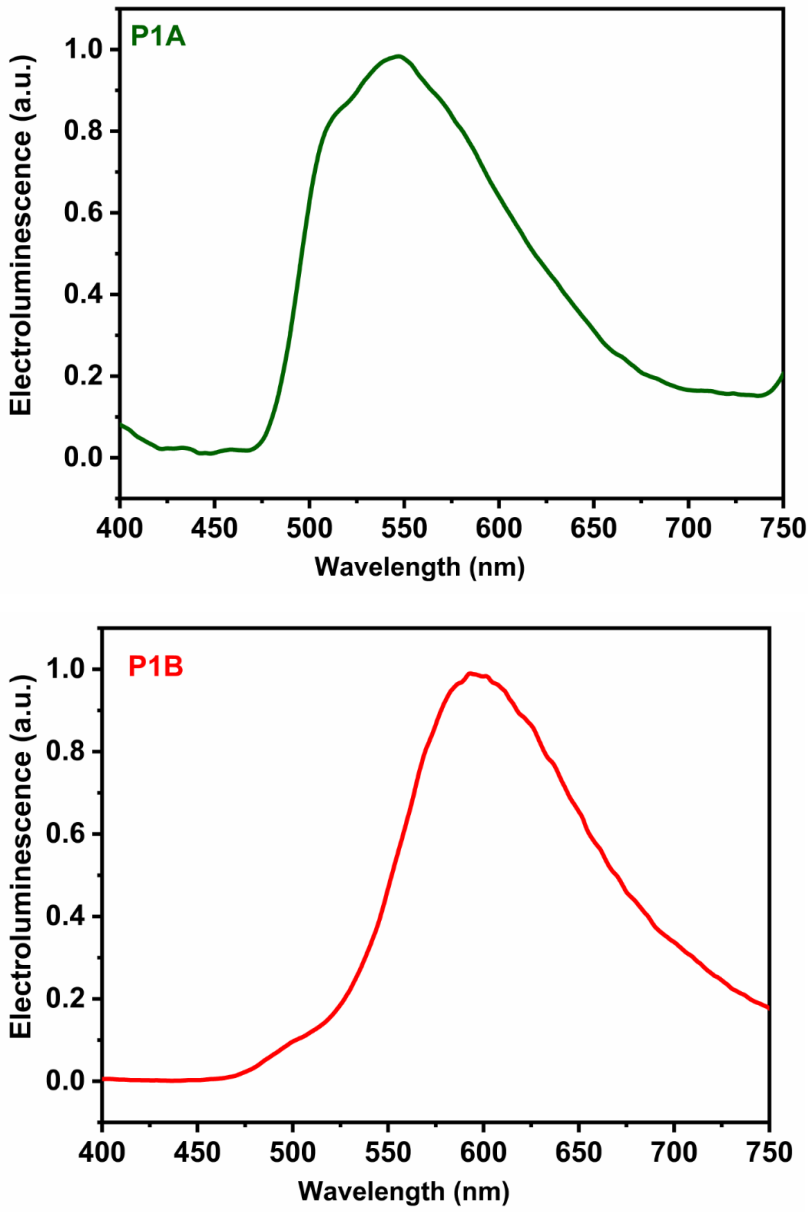

Figure 3.6. Electroluminescence vs wavelength graphs of **P1A** and **P1B**

Figure 3.6. shows electroluminescence versus wavelength graphs. While the maximum wavelength of **P1A** is 545 nm, **P1B** is 595 nm, these results are, as expected, directly related to the colour of the polymers.

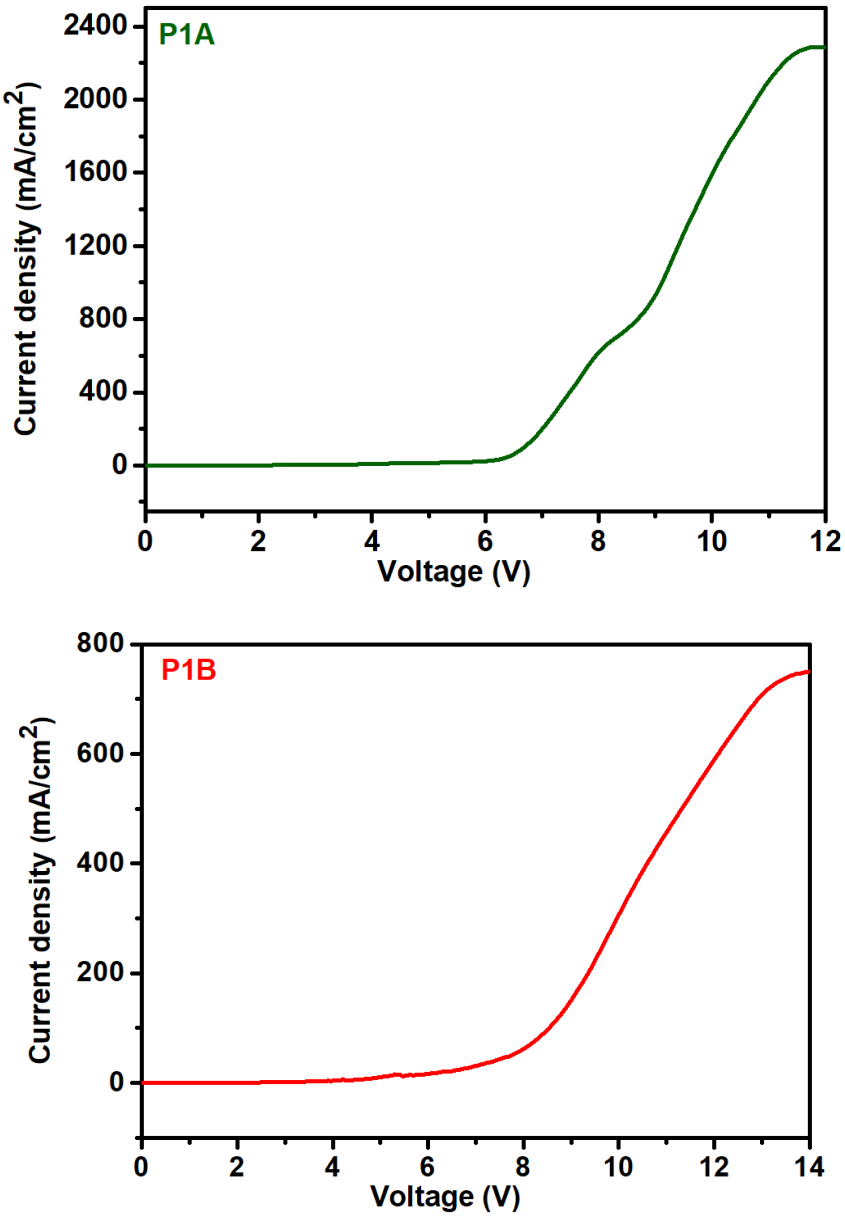

Figure 3.7. Current density vs voltage graphs of **P1A** and **P1B**

As can be seen from the figure, the maximum current density value of **P1A** is up to 2400 mA / cm^2 and the maximum current density value of **P1B** is up to 800 mA / cm^2. As it is understood, there is a significant decrease in the maximum current density values of polymers from **P1A** to **P1B**. This result correlates with the lower quantum yield result of **P1B** with respect to **P1A** obtained from PL measurements.

Although it is generally expected that boron provides higher quantum yields and current density values, in this study the resulting data are quite the opposite [21].

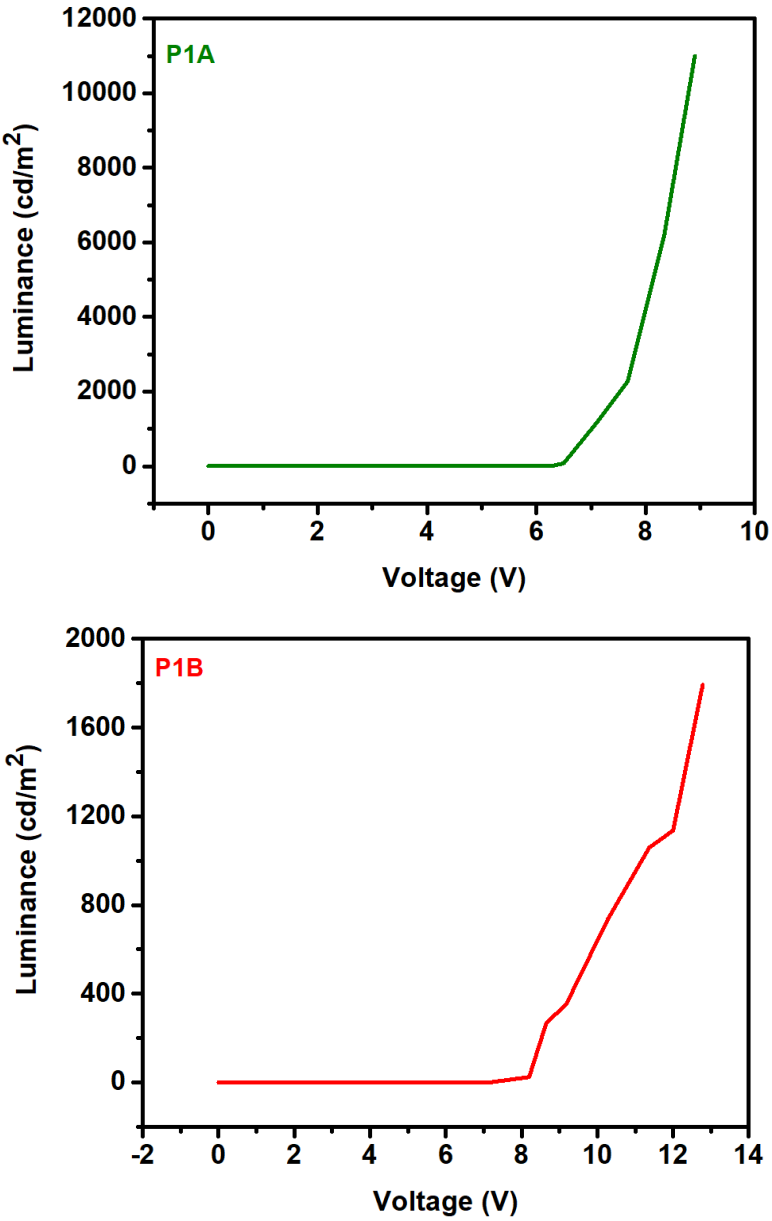

Figure 3.8. Luminescence vs voltage graphs of **P1A** and **P1B**

While the luminescence value of **P1A** goes up to 12000 cd/m^2 at 9 V, the value of **P1B** is 2000 cd/m^2 at 13 V. According to these results, it can be said that decrease in the luminescence from **P1A** to **P1B** is a correlated result with the quantum yields of the corresponding polymers.

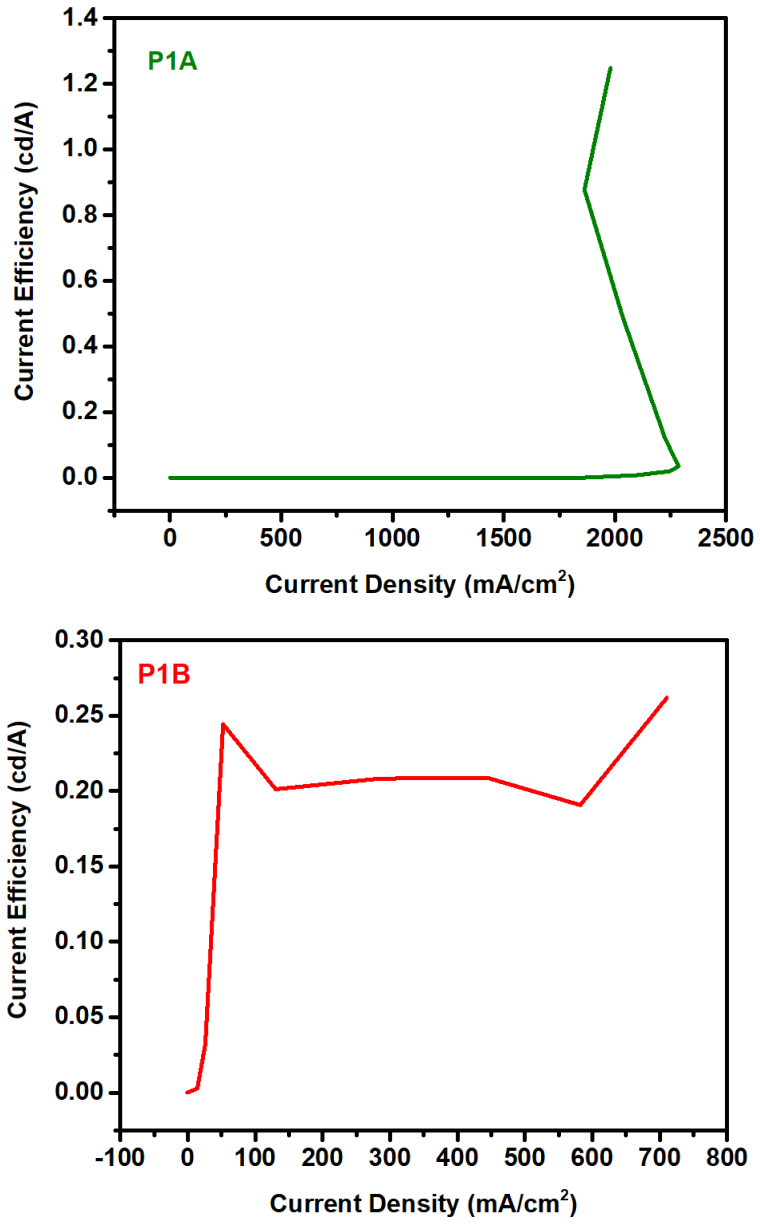

Figure 3.9. Current efficiency vs current density graphs of **P1A** and **P1B**

As can be seen from Figure 3.9., the maximum current efficiency is 1.4 cd/A at 9 V for **P1A** and 0.3 cd/A at 9 V for **P1B**. For both polymers, the device structure is destroyed above 9 V. As can be understood from these graphs, a very significant decrease in current efficiency is observed from **P1A** to **P1B**. The reason for this low efficiency may be due to the inadequacy of the amount of boron unit integrated into the conjugate structure [21].

3.4 GPC Analysis

GPC analyses of polymers were prepared by dissolving 4 mg of polymer in 2 mL of $CHCl_3$ and filtering through polyethersulfone (PES) filters with a pore width of 0.45 microns. As can be seen from Table 3.5., the M_n of **P1A** is 17 kDa, while that of **P1B** is 21 kDa. Again, the data in the same table tells that the M_w of **P1A** is 17 kDa, while that of **P1B** is 21 kDa. PDI values are very close to 1 and this can be explained by the shortness of the polymer chain. Observation of molecular weight increase as a result of boron integration is one of the two important proofs of post-borylation method [21].

Table 3.5. GPC results of **P1A** and **P1B**

	M_n	M_w	PDI
P1A	17 kDa	19 kDa	1.12
P1B	21 kDa	24 kDa	1.14

3.5 Thermal Studies

The thermal properties of polymers were investigated by DSC and TGA methods. Thermal studies, which are very important for this study, are a useful method to determine thermal stability of the polymers. The fact that the polymer containing the boron unit is as stable as the polymer without boron is an indication that the boron unit has maintained its stability while advancing in a good direction in terms of photoelectronic properties. It's possible to comment on the thermal characteristics of polymers revealed by the TGA results performed under nitrogen atmosphere with a heating rate of 10 °C/min between 25 °C - 600 °C. **P1A** shows thermal stability up to 400 °C and a weight loss of 47.38% was observed after this temperature. In **P1B**,

if we ignore the 10% weight loss that appears around 200 °C, it shows thermal stability up to 400 °C like **P1A**, and after this temperature a mass loss of 53.65% observed. Just like the process carried out in TGA analysis, DSC analysis was carried out with nitrogen atmosphere at 10 °C/min heating rate and in the range of 25 °C - 400 °C. Supported these results, it's understood that both boron and boron-free polymers are stable during this thermal range and there are no phase transitions.

CHAPTER 4

CONCLUSION

The boron unit was integrated into the conjugated polymer **P1A** synthesized starting from pyrazine unit, by using a Lewis acid type boron source and its stability was ensured with the phenyl unit with the help of an inorganic salt containing phenyl. Post borylation method, which is a new method of adding desired units after chemical polymerization in the literature, was used in this study. Unlike the classical post borylation method, a different inorganic salt, $AlPh_3$, was used in this study to ensure the stability of the structure, and phenyl integration was successfully achieved. The weight determination of the polymer synthesized **P1A** and modified by the post borylation method **P1B** was made by the GPC technique and number average molecular weight values were 17 and 19 kDa, respectively. Photoluminescence quantum efficiency (PLQY) values are 58% for **P1A** at 510 nm and 76% for **P1B** at 630 nm. Luminance values were recorded as 12000 cd/m^2 for **P1A** and 2000 cd/m^2 for **P1B**. Current efficiencies of **P1A** and **P1B** were recorded as 1.3 cd/A at 9.0 V and 0.3 cd/A at 9.0 V, respectively. In the light of this study, the same post borylation method can be repeated according to different boron unit percentage and the optimum boron percentage can be determined in order to carry the work to a further level. Finding a percentage of boron unit where the stability is as high as possible and the photoelectronic properties reach the maximum level can be realized in the light of this study and can bring a new chapter to the literature on optoelectronic devices containing boron.

REFERENCES

[1] M. Sudhakar, P. I. Djurovich, T. E. Hogen-Esch, and M. E. Thompson, "Phosphorescence quenching by conjugated polymers," *J. Am. Chem. Soc.*, vol. 125, no. 26, pp. 7796–7797, 2003, doi: 10.1021/ja0343297.

[2] A. G. MacDiarmid and A. J. Epstein, "'Synthetic metals': A novel role for organic polymers," *Makromol. Chemie. Macromol. Symp.*, vol. 51, no. 1, pp. 11–28, 1991, doi: 10.1002/masy.19910510104.

[3] T. Higashihara, "Strategic design and synthesis of π -conjugated polymers suitable as intrinsically stretchable semiconducting materials," *Polym. J.*, 2021, doi: 10.1038/s41428-021-00510-1.

[4] H. Peng, X. Sun, W. Weng, and X. Fang, *Polymer Materials for Energy and Electronic Applications*. Elsevier Inc., 2016.

[5] H. Mori, "Development of semiconducting polymers based on a novel heteropolycyclic aromatic framework," *Polym. J.*, 2021, doi: 10.1038/s41428-021-00497-9.

[6] S. J. Hawkes, "Why and When is a Metal?," *Philos. Trans. R. Soc. London, Ser. A*, vol. 86, no. 1, p. 431, 2009, doi: 10.1021/ed100850g.

[7] J. C. Slater, "Band theory," *J. Phys. Chem. Solids*, vol. 8, no. C, pp. 21–25, Jan. 1959, doi: 10.1016/0022-3697(59)90265-3.

[8] K. J. Laws, K. F. Shamlaye, D. Granata, L. S. Koloadin, and J. F. Löffler, "Electron-band theory inspired design of magnesium-precious metal bulk metallic glasses with high thermal stability and extended ductility," doi: 10.1038/s41598-017-03643-7.

[9] J. W. D. Connolly, "The Energy Band Structure of Magnetic Transition Metals*," 1968.

[10] X. Long, Z. Ding, C. Dou, J. Zhang, J. Liu, and L. Wang, "Polymer Acceptor Based on Double B←N Bridged Bipyridine (BNBP) Unit for High-Efficiency All-Polymer Solar Cells," *Adv. Mater.*, vol. 28, no. 30, pp.

6504–6508, 2016, doi: 10.1002/adma.201601205.

[11] M. R. Momeni, L. Shulman, E. Rivard, and A. Brown, “Interplay of donor-acceptor interactions in stabilizing boron nitride compounds: insights from theory,” *Phys. Chem. Chem. Phys.*, vol. 17, no. 25, pp. 16525–16535, 2015, doi: 10.1039/c5cp01993a.

[12] B. Pang *et al.*, “Synthesis of conjugated polymers containing B N bonds with strong electron affinity and extended absorption,” *Polymers (Basel).*, vol. 11, no. 10, 2019, doi: 10.3390/polym11101630.

[13] S. K. Mellerup and S. Wang, “Boron-Doped Molecules for Optoelectronics,” *Trends Chem.*, vol. 1, no. 1, pp. 77–89, 2019, doi: 10.1016/j.trechm.2019.01.003.

[14] Y. Li *et al.*, “8.78% Efficient All-Polymer Solar Cells Enabled by Polymer Acceptors Based on a B←N Embedded Electron-Deficient Unit,” *Adv. Mater.*, vol. 31, no. 44, 2019, doi: 10.1002/adma.201904585.

[15] M. A. Gauthier, M. I. Gibson, and H. A. Klok, “Synthesis of functional polymers by post-polymerization modification,” *Angew. Chemie - Int. Ed.*, vol. 48, no. 1, pp. 48–58, 2009, doi: 10.1002/anie.200801951.

[16] A. Lipp, K. A. Schwetz, and K. Hunold, “Hexagonal boron nitride: Fabrication, properties and applications,” *J. Eur. Ceram. Soc.*, vol. 5, no. 1, pp. 3–9, 1989, doi: 10.1016/0955-2219(89)90003-4.

[17] L. Weber *et al.*, “Syntheses and structures of benzo-bis(1,3,2-diazaboroles) and acenaphtho-1,3,2-diazaboroles,” *Dalt. Trans.*, vol. 48, no. 45, pp. 16911–16921, 2019, doi: 10.1039/c9dt03818c.

[18] J. Yamauchi, M. Tsukada, and S. Watanabe, “First-principles study on energetics of c-BN(001) reconstructed surfaces,” *Phys. Rev. B - Condens. Matter Mater. Phys.*, vol. 54, no. 8, pp. 5586–5603, 1996, doi: 10.1103/PhysRevB.54.5586.

[19] D. Golberg, Y. Bando, C. Tang, and C. Zni, “Boron nitride nanotubes,” *Adv.*

Mater., vol. 19, no. 18, pp. 2413–2432, 2007, doi: 10.1002/adma.200700179.

[20] C. A. Bortolotti *et al.*, "Fast and Selective Post-polymerization Modification of Conjugated Polymers Using Dimethyldioxirane," *Front. Chem. | www.frontiersin.org*, vol. 1, p. 123, 2019, doi: 10.3389/fchem.2019.00123.

[21] D. L. Crossley *et al.*, "Post-polymerization C-H Borylation of Donor-Acceptor Materials Gives Highly Efficient Solid State Near-Infrared Emitters for Near-IR-OLEDs and Effective Biological Imaging," *ACS Appl. Mater. Interfaces*, vol. 9, no. 34, pp. 28243–28249, 2017, doi: 10.1021/acsami.7b08473.

[22] M. Yasa, S. Goker, and L. Toppare, "Selenophene-bearing low-band-gap conjugated polymers: tuning optoelectronic properties via fluorene and carbazole as donor moieties," *Polym. Bull.*, vol. 77, no. 5, pp. 2443–2459, 2020, doi: 10.1007/s00289-019-02872-2.

[23] I. Onk, G. Hizalan, S. C. Cevher, S. O. Hacioglu, L. Toppare, and A. Cirpan, "Multipurpose selenophene containing conjugated polymers for optoelectronic applications," *J. Macromol. Sci. Part A Pure Appl. Chem.*, vol. 54, no. 3, pp. 133–139, 2017, doi: 10.1080/10601325.2017.1265396.

[24] A. Suzuki, "Organoborane coupling reactions (Suzuki coupling)," *Proceedings of the Japan Academy Series B: Physical and Biological Sciences*, vol. 80, no. 8. pp. 359–371, 2004, doi: 10.2183/pjab.80.359.

[25] N. E. Leadbeater and M. Marco, "Rapid and amenable Suzuki coupling reaction in water using microwave and conventional heating," *J. Org. Chem.*, vol. 68, no. 3, pp. 888–892, 2003, doi: 10.1021/jo0264022.

[26] B. H. Ridgway and K. A. Woerpel, "Transmetalation of Alkylboranes to Palladium in the Suzuki Coupling Reaction Proceeds with Retention of Stereochemistry," *J. Org. Chem.*, vol. 63, no. 3, pp. 458–460, 1998, doi: 10.1021/jo970803d.

[27] M. Bernius, M. Inbasekaran, E. Woo, W. Wu, and L. Wujkowski, "Fluorene-based polymers-preparation and applications," vol. 1, pp. 111–116.

[28] M. Inbasekaran, E. Woo, W. Wu, M. Bernius, and L. Wujkowski, "Fluorene homopolymers and copolymers," *Synth. Met.*, vol. 111, pp. 397–401, 2000, doi: 10.1016/S0379-6779(99)00382-3.

[29] A. Donat-bouillud, I. Le, and Y. Tao, "Light-Emitting Diodes from Fluorene-Based," *Chem. Mater*, vol. 12, no. 8, pp. 1931–1936, 2000.

[30] R. Xia, G. Heliotis, Y. Hou, and D. D. C. Bradley, "Fluorene-based conjugated polymer optical gain media," *Org. Electron.*, vol. 4, no. 2–3, pp. 165–177, 2003, doi: 10.1016/j.orgel.2003.08.009.

[31] K. Hoffert, R. J. Durand, S. Gauthier, F. Robin-Le Guen, and S. Achelle, "Synthesis and Photophysical Properties of a Series of Pyrazine-Based Push-Pull Chromophores," 2017, doi: 10.1002/ejoc.201601204.

[32] E. V. Verbitskiy *et al.*, "Synthesis, photophysical and nonlinear optical properties of [1,2,5]oxadiazolo[3,4-b]pyrazine-based linear push-pull systems," *J. Photochem. Photobiol. A Chem.*, vol. 404, no. June 2020, 2021, doi: 10.1016/j.jphotochem.2020.112900.

[33] S. Sudheendran Swayamprabha *et al.*, "Approaches for Long Lifetime Organic Light Emitting Diodes," *Adv. Sci.*, vol. 8, no. 1, pp. 1–29, 2021, doi: 10.1002/advs.202002254.

[34] T. Chimiche, "Synthesis of Heterocycles for OLED Applications," 2015.

[35] D. Yan, H. Wang, and B. Du, "Organic Heterostructure in Electronic Devices," *Introd. to Org. Semicond. Heterojunctions*, pp. 1–6, 2010, doi: 10.1002/9780470825969.ch1.

[36] D. Fichou and G. Horowitz, "Molecular and Polymer Semiconductors, Conductors, and Superconductors: Overview," in *Encyclopedia of Materials: Science and Technology*, Elsevier, 2001, pp. 5748–5757.

[37] G. Zissis and P. Bertoldi, *2014 Status Report on Organic Light Emitting Diodes (OLED)*. 2014.

[38] G. Tuttle, "Organic light emitting devices (OLEDs) and Structurally integrated photoluminescence based chemical and biological sensors excited by OLEDs," *Small*, p. 132, 2005.

[39] R. Ma, "Organic light emitting diodes (OLEDS)," *Handb. Vis. Disp. Technol.*, vol. 2, no. June, pp. 1209–1221, 2012, doi: 10.1007/978-3-540-79567-4_6.6.1.

[40] Z. Wang, "Design of High Performance Organic Light Emitting Diodes," p. 104, 2012.

[41] A. Islam, M. Rabbani, M. H. Bappy, M. A. R. Miah, and N. Sakib, "A review on fabrication process of organic light emitting diodes," *2013 Int. Conf. Informatics, Electron. Vision, ICIEV 2013*, 2013, doi: 10.1109/ICIEV.2013.6572656.

[42] Y. Cai, "Organic light emitting diodes (OLEDs) and OLED-based structurally integrated optical sensors," *Grad. Theses Diss.*, 2010, [Online]. Available: http://lib.dr.iastate.edu/etd/11488.

[43] Z. Wang, "Design of High Performance OLED Diodes," 2012.

[44] T. Z. Forbes, "Luminescence," *Encycl. Earth Sci. Ser.*, pp. 835–838, 2018, doi: 10.1180/minmag.1999.063.2.10.

[45] R. Capelletti, "178 Luminescence," pp. 178–189, 2005.

[46] G. Blasse and A. Bril, "Luminescence phenomena in compounds with fergusonite structure," *J. Lumin.*, vol. 3, no. 2, pp. 109–131, 1970, doi: 10.1016/0022-2313(70)90011-6.

[47] C. Moretti, X. Tao, L. Koehl, and V. Koncar, *Electrochromic textile displays for personal communication*. Elsevier Ltd, 2016.

[48] M. Leskelä, W. M. Li, M. Ritala, and A. Z. M. S. Rahman, "Electroluminescent Phosphors ☆," *Ref. Modul. Mater. Sci. Mater. Eng.*, no.

August 2017, pp. 1–9, 2018, doi: 10.1016/b978-0-12-803581-8.10536-3.

[49] R. M. Christie, *Fluorescent dyes*, vol. 1. Woodhead Publishing Limited, 2011.

[50] F. Wang, X. K. Liu, and F. Gao, *Fundamentals of solar cells and light-emitting diodes*. Elsevier Inc., 2019.

[51] A. Srivastava *et al.*, *Characterizations of nanoscale two-dimensional materials and heterostructures*. INC, 2020.

[52] Q. Zhu, *In situ planar optical sensors for sediment diagenesis study*, 3rd ed. Elsevier Ltd., 2019.

[53] H. B. Bebb and E. W. Williams, "Photoluminescence I: Theory," *Semicond. Semimetals*, vol. 8, no. C, pp. 181–320, 1972, doi: 10.1016/S0080-8784(08)62345-5.

[54] S. A. E. Marras, F. R. Kramer, and S. Tyagi, "Efficiencies of fluorescence resonance energy transfer and contact-mediated quenching in oligonucleotide probes.," *Nucleic Acids Res.*, vol. 30, no. 21, pp. 1–8, 2002, doi: 10.1093/nar/gnf121.

[55] I. Tanaka, Y. Tabata, and S. Tokito, "Förster and Dexter energy-transfer processes in fluorescent BAlq thin films doped with phosphorescent Ir(ppy)3 molecules," *J. Appl. Phys.*, vol. 99, no. 7, 2006, doi: 10.1063/1.2185835.

[56] A. Cravcenco, C. Ye, J. Gräfenstein, and K. Börjesson, "Interplay between Förster and Dexter Energy Transfer Rates in Isomeric Donor-Bridge-Acceptor Systems," *J. Phys. Chem. A*, vol. 124, no. 36, pp. 7219–7227, 2020, doi: 10.1021/acs.jpca.0c05035.

[57] J. K. Borchardt, "Developments in organic displays," *Mater. Today*, vol. 7, no. 9, pp. 42–46, 2004, doi: 10.1016/S1369-7021(04)00401-8.

[58] S. J. Zou, Y. Shen, F. M. Xie, J. De Chen, Y. Q. Li, and J. X. Tang, "Recent advances in organic light-emitting diodes: Toward smart lighting and displays," *Mater. Chem. Front.*, vol. 4, no. 3, pp. 788–820, 2020, doi:

10.1039/c9qm00716d.

[59] H. W. Chen, J. H. Lee, B. Y. Lin, S. Chen, and S. T. Wu, “Liquid crystal display and organic light-emitting diode display: present status and future perspectives,” *Light Sci. Appl.*, vol. 7, no. 3, p. 17168, 2018, doi: 10.1038/lsa.2017.168.

[60] H. Cho *et al.*, “White organic light-emitting diode (OLED) microdisplay with a tandem structure,” *J. Inf. Disp.*, vol. 20, no. 4, pp. 249–255, 2019, doi: 10.1080/15980316.2019.1671240.

[61] C. W. Tang and S. A. Vanslyke, “Organic electroluminescent diodes,” *Appl. Phys. Lett.*, vol. 51, no. 12, pp. 913–915, 1987, doi: 10.1063/1.98799.

[62] S. Kappaun, C. Slugovc, and E. J. W. List, “Phosphorescent organic light-emitting devices: Working principle and iridium based emitter materials,” *Int. J. Mol. Sci.*, vol. 9, no. 8, pp. 1527–1547, 2008, doi: 10.3390/ijms9081527.

[63] C. Zhu, “OLED Technology Research Progress and Prospects for Future Application,” vol. 6, no. 09, pp. 77–79, 2017, [Online]. Available: www.ijert.org.

[64] Q. Huang *et al.*, “Donor-acceptor nanoensembles based on boron nitride nanotubes,” *Adv. Mater.*, vol. 19, no. 7, pp. 934–938, 2007, doi: 10.1002/adma.200602058.

[65] X. Lan, Q. Li, Y. Zhang, Q. Li, L. Ricardez-Sandoval, and G. Bai, “Engineering donor-acceptor conjugated organic polymers with boron nitride to enhance photocatalytic performance towards visible-light-driven metal-free selective oxidation of sulfides,” *Appl. Catal. B Environ.*, vol. 277, no. March, 2020, doi: 10.1016/j.apcatb.2020.119274.

[66] Y. Fujimoto and S. Saito, “Effects of strain on carbon donors and acceptors in hexagonal boron nitride monolayers,” *Phys. Rev. B*, vol. 93, no. 4, pp. 1–7, 2016, doi: 10.1103/PhysRevB.93.045402.

[67] A. John *et al.*, "Doubly boron-doped pentacenes as emitters for OLEDs," *J. Mater. Chem. C*, vol. 6, no. 40, pp. 10881–10887, 2018, doi: 10.1039/c8tc03954b.

[68] M. Caliskan, M. C. Erer, S. T. Aslan, Y. A. Udum, L. Toppare, and A. Cirpan, "Narrow band gap benzodithiophene and quinoxaline bearing conjugated polymers for organic photovoltaic applications," *Dye. Pigment.*, vol. 180, no. April, p. 108479, 2020, doi: 10.1016/j.dyepig.2020.108479.

[69] Y. Li *et al.*, "Synthesis of B←N embedded indacenodithiophene chromophores and effects of bromine atoms on photophysical properties and energy levels," *Tetrahedron*, vol. 74, no. 32, pp. 4308–4314, 2018, doi: 10.1016/j.tet.2018.06.035.

[70] S. N. Inamdar, P. P. Ingole, and S. K. Haram, "Determination of band structure parameters and the quasi-particle gap of CdSe quantum dots by cyclic voltammetry," *ChemPhysChem*, vol. 9, no. 17, pp. 2574–2579, 2008, doi: 10.1002/cphc.200800482.

[71] S. Pluczyk, M. Vasylieva, and P. Data, "Using Cyclic Voltammetry, UV-Vis-NIR, and EPR Spectroelectrochemistry to Analyze Organic Compounds," *J. Vis. Exp.*, no. 140, pp. 1–13, 2018, doi: 10.3791/56656.

[72] Y. Adachi, Y. Ooyama, Y. Ren, X. Yin, F. Jäkle, and J. Ohshita, "Hybrid conjugated polymers with alternating dithienosilole or dithienogermole and tricoordinate boron units," *Polym. Chem.*, vol. 9, no. 3, pp. 291–299, 2018, doi: 10.1039/c7py01790a.

[73] A. Erbe *et al.*, *How to probe structure, kinetics, and dynamics at complex interfaces in situ and operando by optical spectroscopy*. Elsevier, 2018.

[74] J. T. Torvik, "Dopants in GaN," *III-Nitride Semicond. Electr. Struct. Defects Prop.*, pp. 17–49, 2000, doi: 10.1016/b978-044450630-6/50003-9.

[75] G. T. Tigineh and L. K. Liu, "Solvatochromic photoluminescence investigation of functional Schiff-bases: A systematic study of substituent

effects," *J. Photochem. Photobiol. A Chem.*, vol. 338, pp. 161–170, 2017, doi: 10.1016/j.jphotochem.2017.02.001.

[76] S. C. Cevher *et al.*, "A comprehensive study: Theoretical and experimental investigation of heteroatom and substituent effects on frontier orbitals and polymer solar cell performances," *J. Polym. Sci.*, vol. 58, no. 19, pp. 2792–2806, 2020, doi: 10.1002/pol.20200513.

APPENDICES

A. NMR-DSC-TGA results

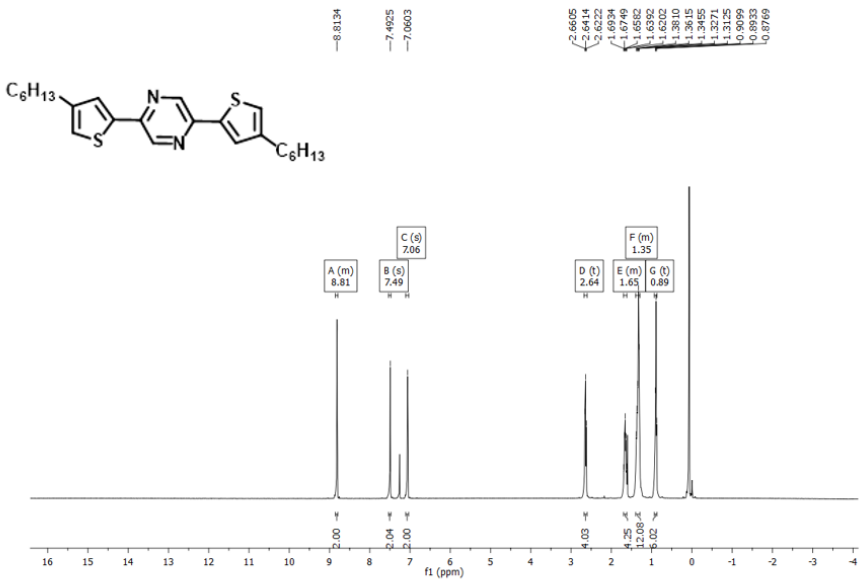

^{1}H NMR result of 2,5-di(3-hexylthiophen-2-yl)pyrazine

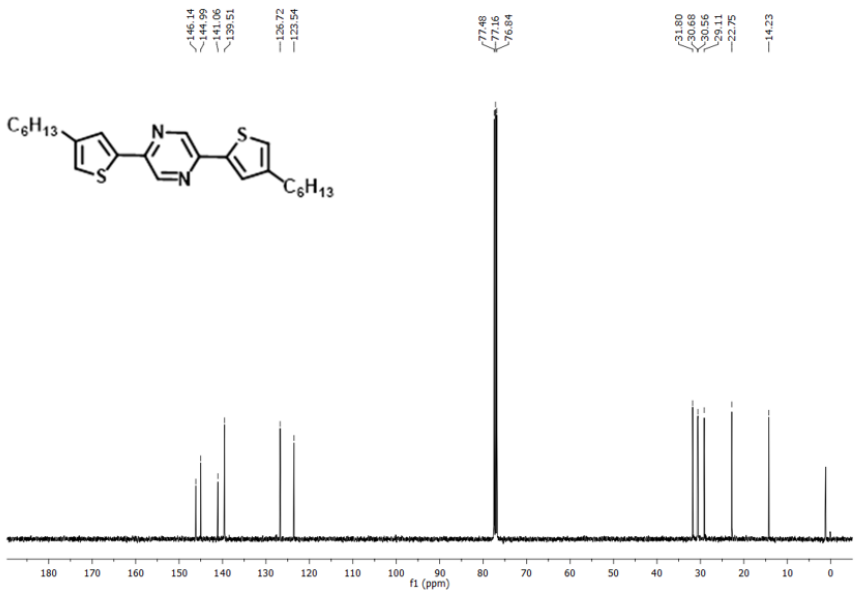

^{13}C NMR result of 2,5-di(3-hexylthiophen-2-yl)pyrazine

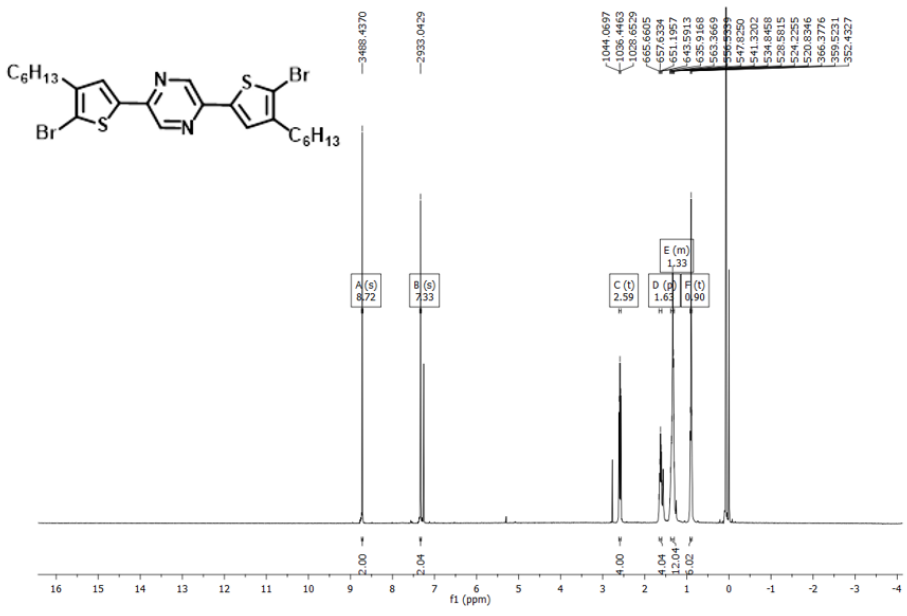

^{1}H NMR result of 2,5-bis-(5-bromo-4-hexylthiophen-2-yl)pyrazine

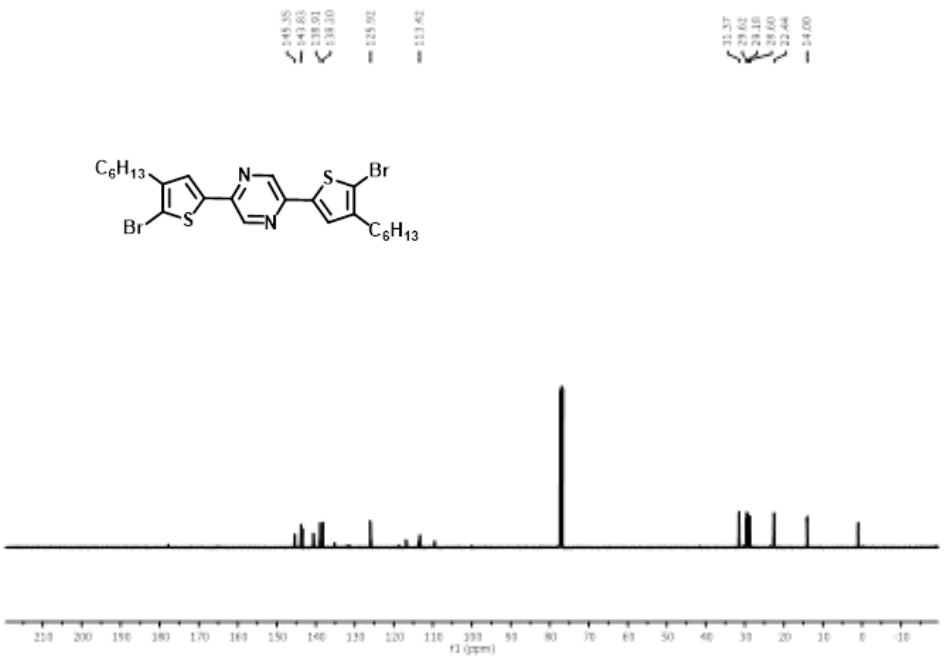

^{13}C NMR result of 2,5-bis-(5-bromo-4-hexylthiophen-2-yl)pyrazine

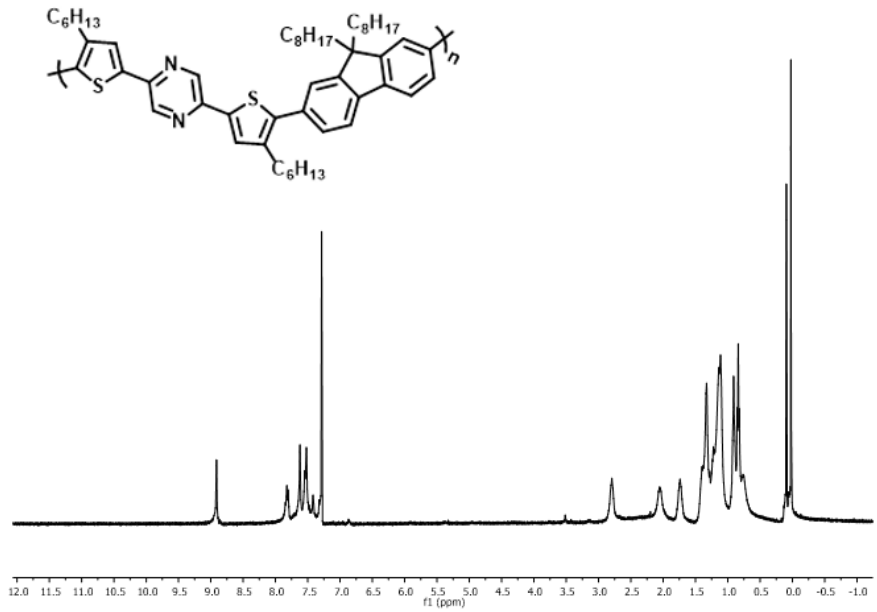

^{1}H NMR result of P1A

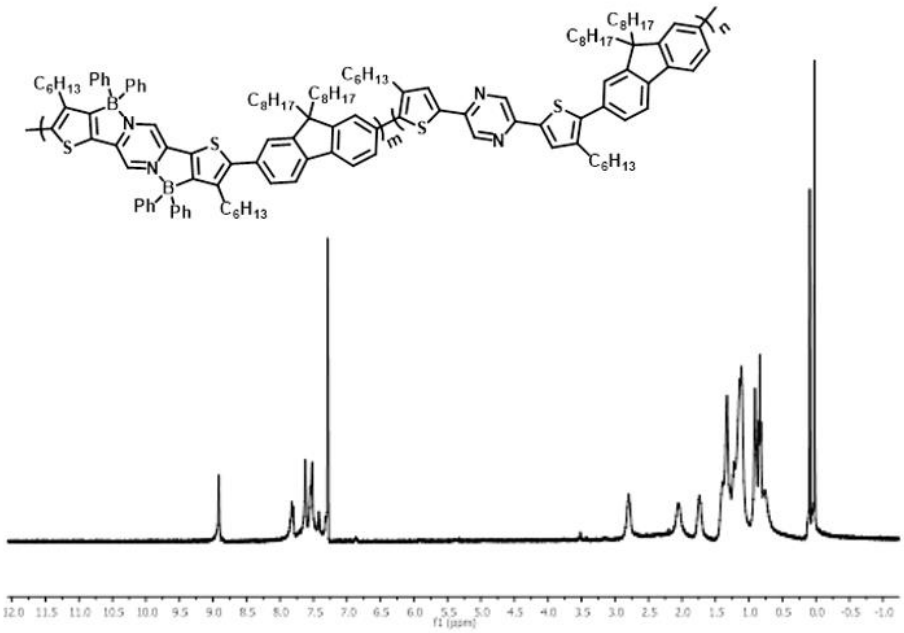

^{1}H NMR result of P1B

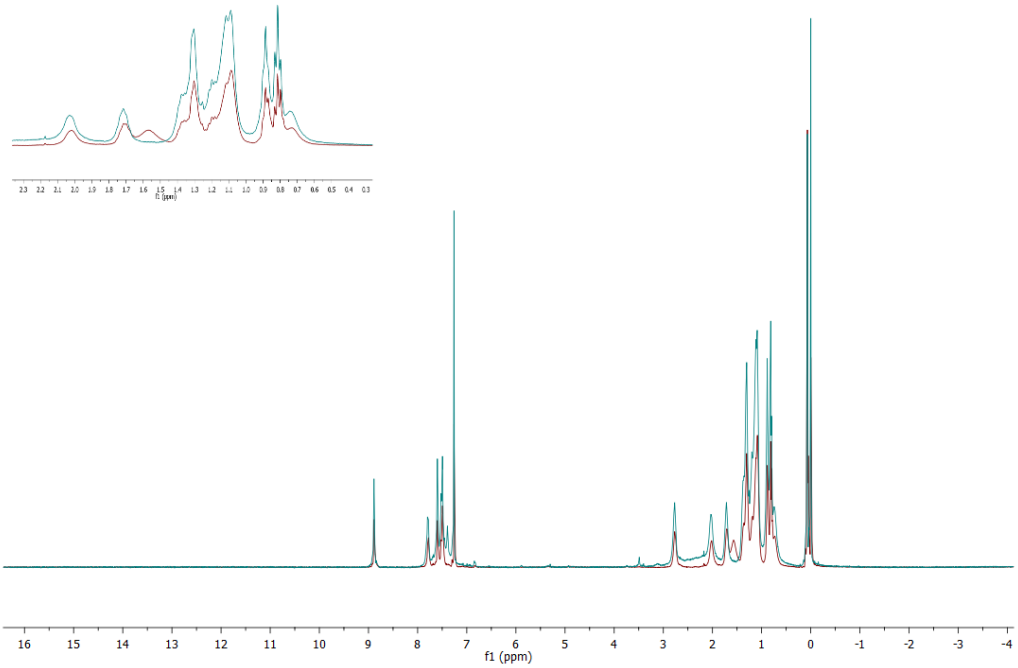

Comparison of P1A and P1B

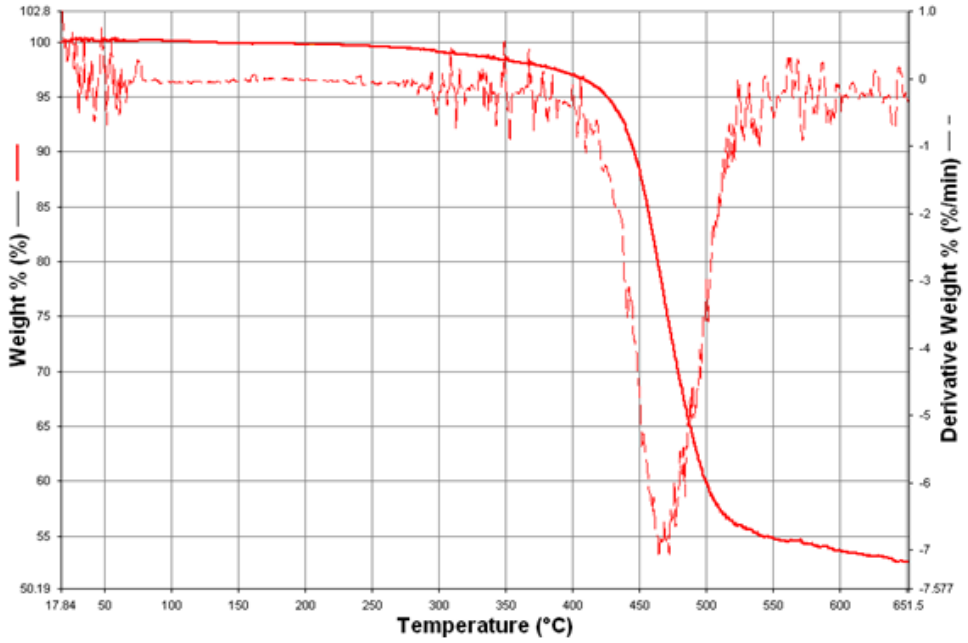

TGA result of P1A

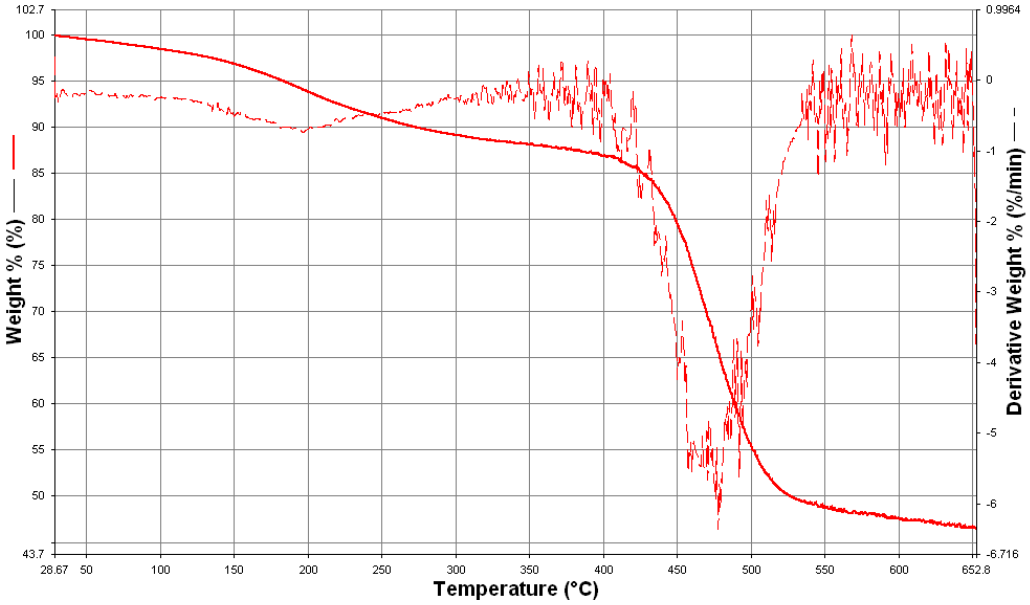

TGA result of P1B

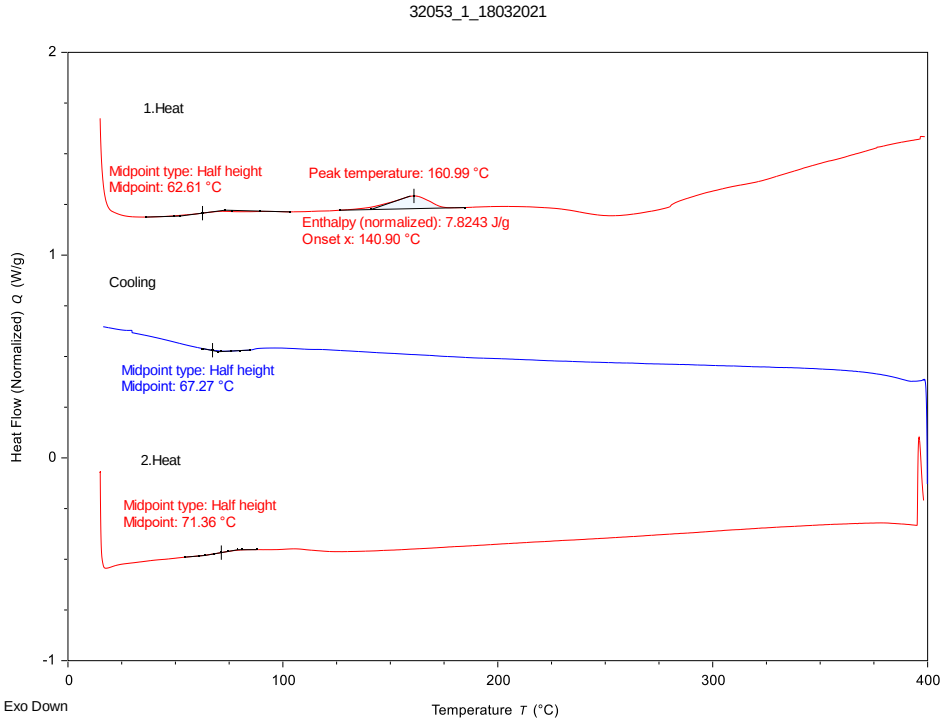

DSC result of P1A

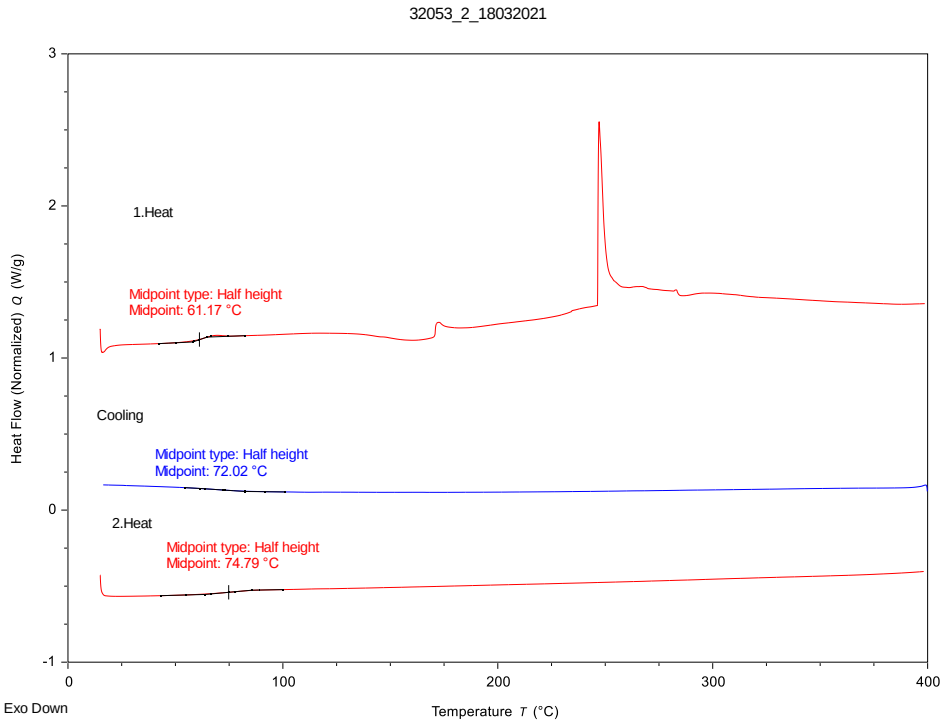

DSC result of P1B